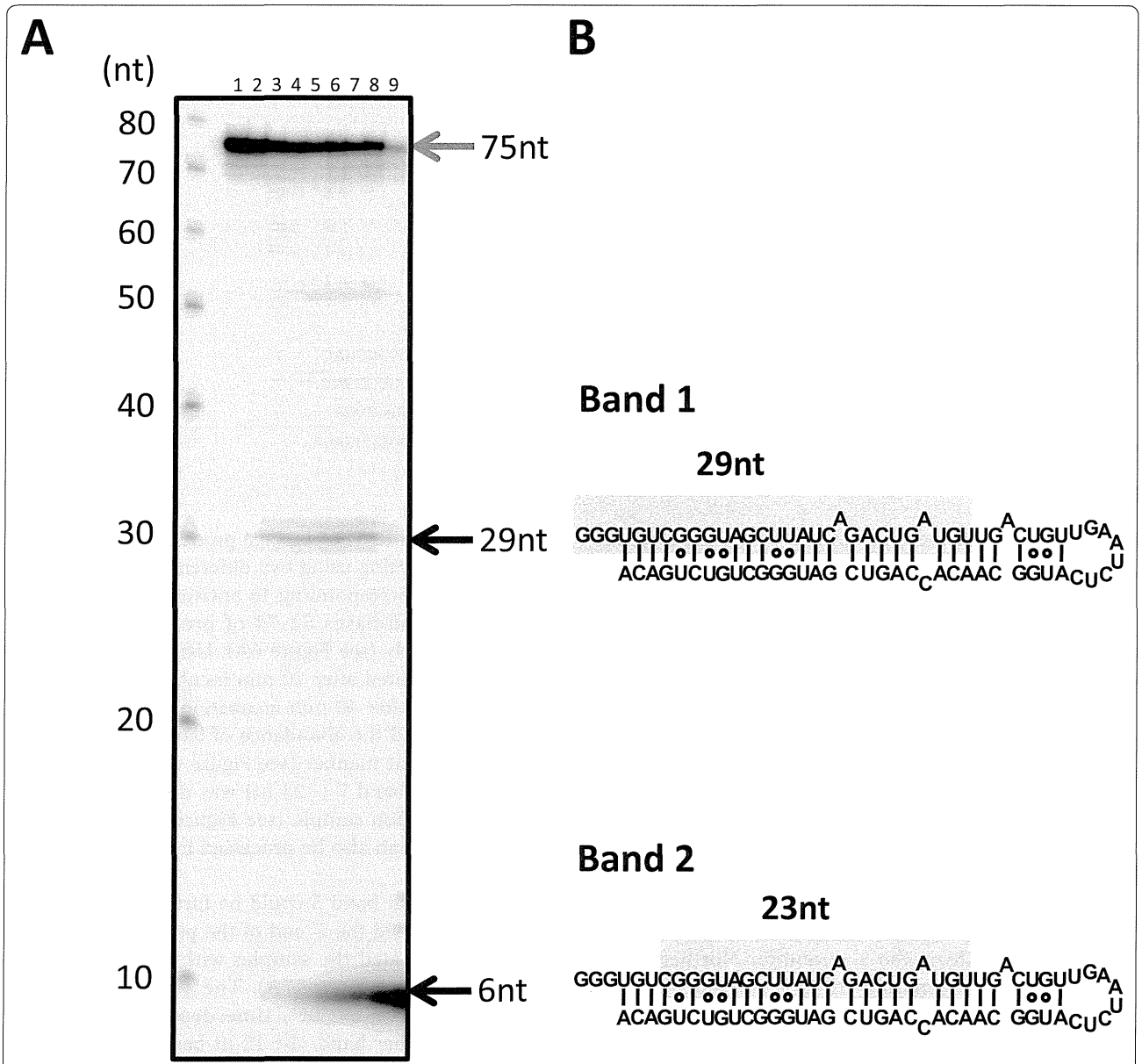

Figure 4 Two-step processing of the 5'-end labelled RNA-I by recombinant DICER protein. (**A**) *In vitro* processing of the 5'-end labelled RNA-I by rDICER protein. 5'-end labelled RNA-I RNAs were incubated without rDICER for 120 min (lane 1) and with rDICER for the following time points (0, 10, 20, 30, 40, 50, 60 and 120 min; lane 2-9 respectively). The processing reaction was faster than the results of Figure 3B because the amount of RNA substrate in this reaction mixture was less. The RNA products less than 10 nt look stacked at the end of the gel because of the difficulty in separating efficiently, even at 7.5 M urea denaturing 20% polyacrylamide sequence gel. This experiment was repeated and replicated consistently. M: decade marker. (**B**) Sequences of band 1 and 2 in Figure 3B identified from Figure 4A and Table 1. Sequences highlighted in gray are 29-nt (band 1) and 23-nt RNA (band 2) from the 5' strand, respectively.

dsRNAs remains unclear, it seems likely that they have diverse 5' and 3' structures. Our results indicate DICER tolerance for 5' substrate overhang, potentially increasing the range of small RNA substrates that DICER can process. Recently, it was reported that the AGO2 protein could bind not only siRNAs and miRNAs but longer RNAs and pre-miRNAs [22,40]. However, most endogenous AGO2 proteins bind miRNAs [41] and the RISC requires 3' overhangs for the dsRNA incorporation [3,42]. As this research shows, DICER could process pre-miRNAs, longer dsRNAs and hairpin RNAs with 5' overhangs into dsRNA with 3' overhangs, which might be subsequently loaded with canonical length to the RISC. Further experimentation is required to connect our findings with the AGO loading mechanism.

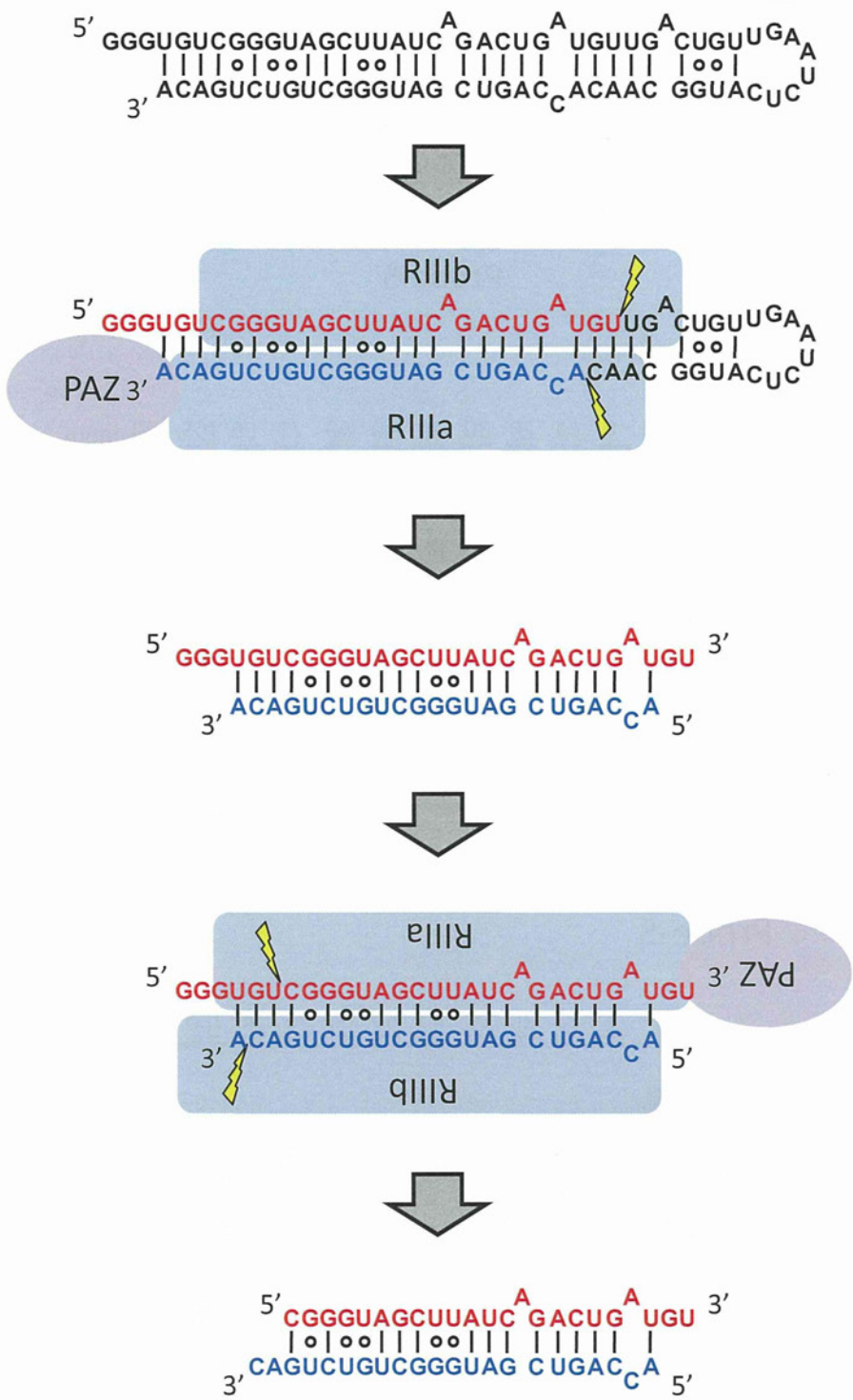

Figure 5 Model of the two-step processing of hairpin RNA with 5′ overhangs (RNA-I) by DICER protein. *rDICER processes hairpin RNA with 5′ overhangs (RNA-I) to dsRNA with 29 nt-5′ strand and 23 nt-3′ strand after the first cleavage reaction and releases once from the binding site. Then, the dsRNA is bound in the inverse direction with the same or different rDICER molecule and is measured after the anchoring 3′ end of the 29-nt strand to generate dsRNA with 23 nt cleaved from the 29-nt strand and 22 nt cleaved from the 23-nt strand. "PAZ" domain of rDICER colored purple; "RIIIa" and "RIIIb" domain of rDICER colored blue. Lightning marks indicate the cleavage sites in the RNA.*

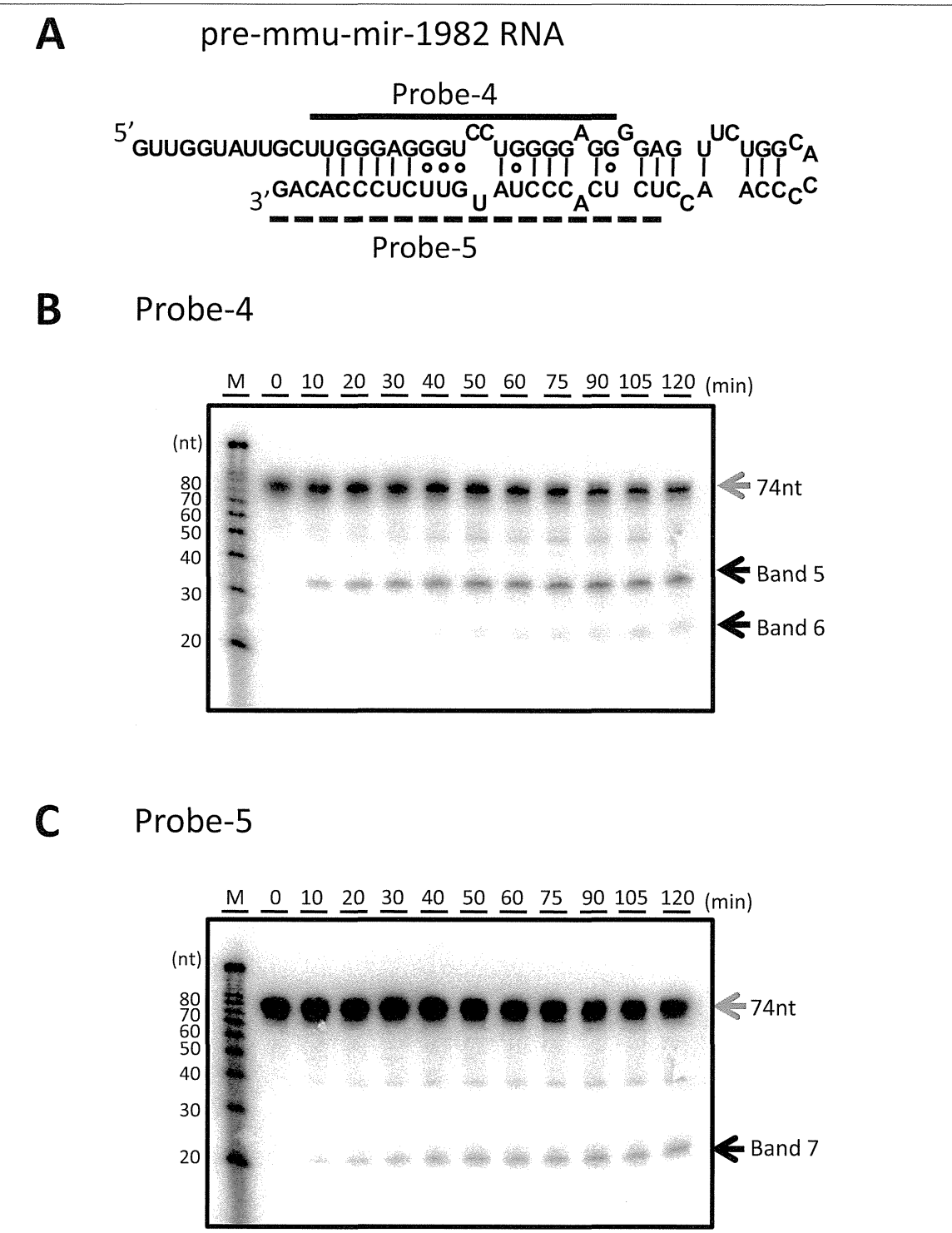

Figure 6 Processing of pre-mmu-mir-1982 RNA by recombinant DICER protein. (**A**) Pre-mmu-mir-1982 RNA and probes used in this study. The secondary structure was predicted using the CentroidFold program [49]. The solid line shows the position of probe-4 and the dashed line shows the position of probe-5. (**B-C**) Time-course analysis of the processing of pre-mmu-mir-1982 RNA by the rDICER protein. pre-mmu-mir-1982 RNAs were incubated with rDICER *in vitro* for the indicated time points (0, 10, 20, 30, 40, 50, 60, 75, 90, 105 and 120 min). The RNAs processed by rDICER were detected using probe-4 (**B**), probe-5 (**C**) by Northern blotting. The gray arrow shows the band of unprocessed RNA and the black arrow shows the bands of small RNA processed from the 5' strand and 3' strand of pre-mmu-mir-1982 RNA respectively. M: decade marker.

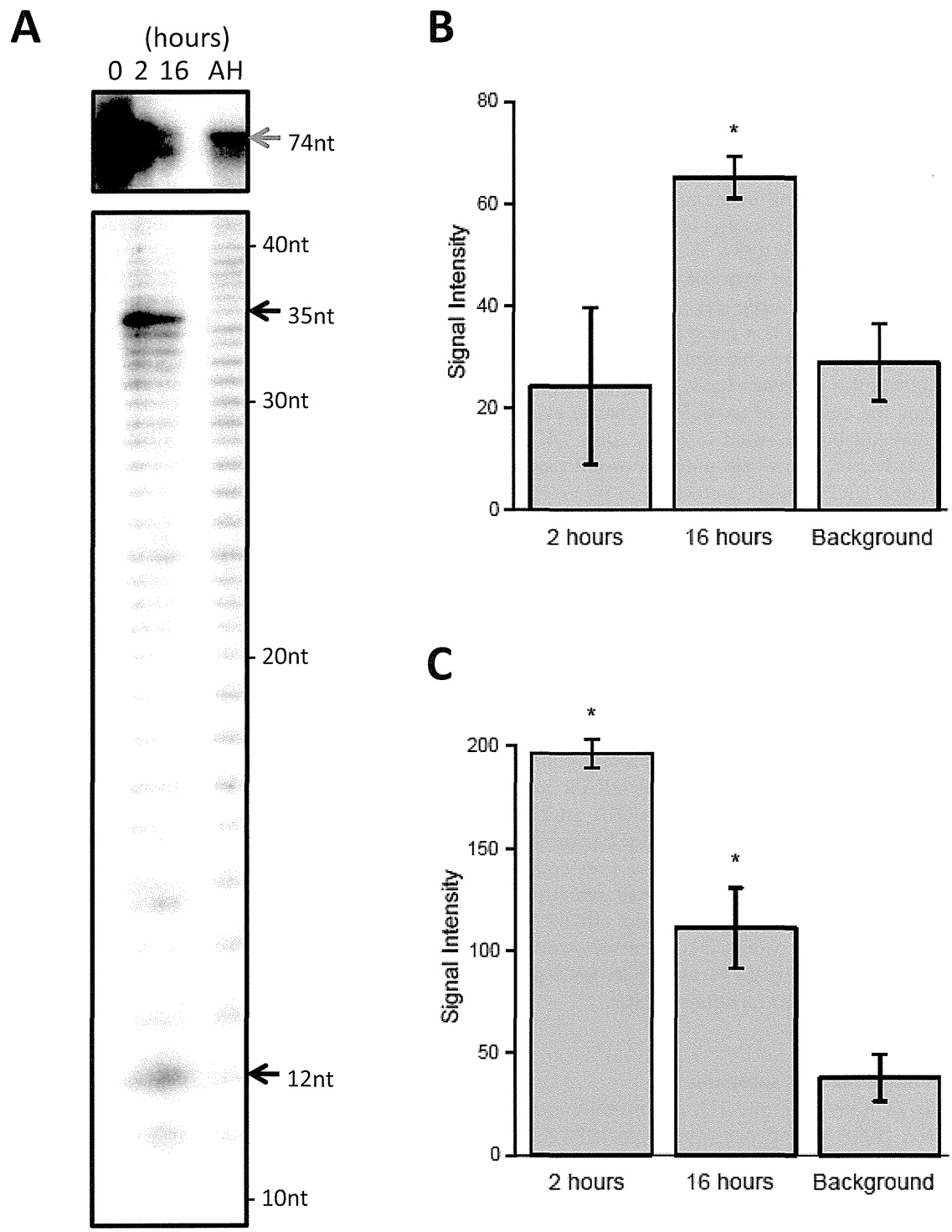

Figure 7 Two-step processing of the 5'-end labelled pre-mmu-mir-1982 RNA by recombinant DICER protein. (**A**) *In vitro* processing of the pre-mmu-mir-1982 RNA by the rDICER protein at a longer incubation time. 5' labelled pre-mmu-mir-1982 RNAs were incubated with rDICER for 0, 2 and 16 hours. The gray arrow shows the band of unprocessed RNA and the black arrow shows the bands of small RNA processed from pre-mmu-mir-1982 RNA. AH: the alkaline hydrolysis ladder of pre-mmu-mir-1982 RNA. The size of each band was determined by the AH ladder. (**B-C**) The signal intensities were quantified from the 12 nt (**B**) and 35 nt (**C**) bands in Figure 7A. These plots show average values bracketed by s.e.m. error bars; calculated from two independent experiments. Background refers to the signal intensity of the same sized band in the AH lane. The p-value was calculated using a simple t-test for each time point (2 hrs and 16 hrs) relative to the background. Significant differences ($p < 0.05$) in signal intensities are denoted with an asterisk. The significant calculated p-values are as follows: the 12-nt band at 16 hours, $p = 0.017$; the 35-nt band at 2 hours, $p = 0.0073$; and the 35-nt band at 16 hours, $p = 0.024$.

Conclusions

We show human rDICER recognizes and processes a hairpin RNA bearing a trinucleotide-5' overhang, and the two-step cleavage by rDICER forms canonical miRNA duplexes from the hairpin RNAs. It indicates that human rDICER functions as a molecular ruler by anchoring the 3' end of both the hairpin RNA with 5' overhangs and the 5' strand in the intermediate duplex. Moreover, an endogenously-expressed pre-miRNA with 5' overhangs, pre-mmu-mir-1982, also can be utilized as a substrate of rDICER and processed into a canonical miRNA duplex by the two-step cleavage reaction. While pre-mmu-mir-1982 RNA is a naturally expressed pre-miRNA [33,35], this 5'-overhanged structure is not a suitable substrate for nuclear export by Exportin-5 [43] and, assuming the absence of possible alternative export pathways, may not be presented to cytoplasmic DICER in the cells. However, it is worth noting a recent report, that mammalian DICER might be located in the nucleus and associate with ribosomal DNA chromatin [44]. We have also observed human DICER localized in both cytoplasm and nucleus (unpublished data, Ando *et al.*). These findings raise the intriguing possibility that nuclear DICER could process hairpin RNA with 5'-overhangs, like pre-mmu-mir-1982 RNA.

The two-step cleavage of a hairpin RNA with 5' overhangs shows that rDICER can release dsRNAs after the first cleavage and binds them again in the inverse direction for a second cleavage. The DICER protein's ability to release and bind dsRNA again indicates DICER could be capable of binding and processing dsRNA multiple times during short RNA maturation. DICER has recently been linked to the processing of diverse non-coding RNA precursors with as-yet undetermined structures. The experiments performed above suggest DICER has considerable flexibility in processing precursors, contributing to an ability to generate various short RNA products for incorporation into functional RISCs.

Methods

Preparation of hairpin RNA substrates

Pre-hsa-mir-21 RNA (pre-mir-21), pre-miRNA mimic hairpin RNA (RNA-I) and pre-mmu-mir-1982 RNA used in this study were generated by *in vitro* transcription using the Ampliscribe T7 High Yield Transcription kits (Epicentre) according to manufacturer's instructions. We made double-stranded DNA templates with T7 RNA polymerase promoter sequence by overlap-PCR using the following oligonucleotide pair; pre-mir-21-sense 5'-taatacgactcactatagAGCTTATCAGACTGATGTTGACTG-3' and pre-mir-21-antisense 5'-ACAGCCCATCGACTGGTGTTGCCATGAGATTCAACAGTCAACATC-3', RNAI-sense 5'-taatacgactcactatagggTGTCGGGTAGCTTATCAGACTGATGTTGA-3' and RNAI-antisense 5'-TGTCAGACAGCCCATCGACTGGTGTTGCCATGAGATTCAACAGTCAACA-3', pre-mmu-mir-1982-sense 5'-taatacgactcactataGTTGGTATTGCTTGGGAGGGTCCTGGGGAGGGGAGTT-3' and pre-mmu-mir-1982-antisense 5'-CTGTGGGAGAACATAGGGTGAGAGGTTGGGGTGCCAGAACTCCCCTCCCCA-3'. The overlapped sequences are underlined and the lower-case characters show the sequence of the T7 RNA polymerase promoter. *In vitro* transcription reactions were performed at 37°C overnight. Transcripts were run on 10% denaturing polyacrylamide gels in 0.5x TBE (45 mM Tris-borate, 1 mM EDTA), gel-excised, eluted from the gel in 1 M NaCl at 4°C overnight, and precipitated with ethanol. The pellet was resuspended in an appropriate volume of water and stored into the freezer at -30°C. Before use, RNA substrates were heated to 70°C for 5 min and then slowly cooled to room temperature.

Affinity purification of recombinant FLAG-DICER fusion proteins

We assembled a full-length cDNA of human DICER1 protein from HeLa total RNA. This cDNA sequence was identical to the coding sequence cited in the Swiss-Prot Protein Database (Swiss-Prot) [Swiss-Prot: Q9UPY3]. N-terminally FLAG-tagged human DICER1 protein was purified from 293T cells transfected with the plasmid pCA-FLAG-DICER1. This vector contained the full-length human DICER1 protein FLAG-tagged at the amino terminus in a pCA-FLAG-DEST vector [45]. We purified the recombinant FLAG-DICER1 fusion protein (rDICER) using ANTI-FLAG M2-Agarose Affinity Gel (Sigma) and eluted by 0.1 M Glycine-HCl (pH3.5). Then, the eluate was neutralized by Tris-HCl (pH8.0). The average yield was 50-100 μg of the active form of rDICER protein from 1×10^8 culture cell. Purified rDICER protein was detected by Coomassie Brilliant Blue (CBB) staining and Western blotting using anti-DICER (H212, Santa Cruz) antibody to check for successful homogenous purification (see Figures 1A and 1B). The contamination of known DICER-binding proteins in rDICER samples was checked by Western blotting using anti-FLAG (M2, Sigma), anti-AGO2 (07-590, Upstate) and anti-TRBP (ab42018, Abcam) antibody, respectively (see Figure 1C).

Processing of RNA substrates using recombinant DICER enzyme

The affinity-purified rDICER protein (2 pmol) was incubated with 45 pmol of RNA substrates (pre-mir-21 RNA, RNA-I or pre-mmu-mir-1982 RNA) in 1x reaction buffer (300 mM NaCl, 50 mM Tris-HCl, 20 mM

HEPES, 5 mM $MgCl_2$, pH 9.0) and 40 units of RNase-OUT (Invitrogen). These mixtures were incubated at 37°C for the indicated times. The reactions were purified by phenol-chloroform extraction followed by sodium acetate-ethanol precipitation at -20°C. The RNA pellet was resuspended in water at a final concentration of approximately 1 pmol/μl.

Northern blotting

rDICER-processed RNAs (1 pmol) were separated on 7 M urea-denaturing 20% polyacrylamide gels, then blotted onto Hybond-N+ membranes (GE Healthcare) using a Trans-Blot SD Semi-Dry Transfer Cell (Bio-Rad). Hybridization was performed in Church buffer (0.5 M $NaHPO_4$, pH 7.2, 1 mM EDTA and 7% SDS) containing 10^6 c.p.m./ml of each ^{32}P-labelled probe for 14 h. The membranes were washed in 2x SSC, and the signals were detected by autoradiography. All experiments were repeated and replicated consistently.

The probe sequences in this study were as follows: probe-1 (5'-TCAACATCAGTCTGATAAGCTA-3'), probe-2 (5'-ACAGCCCATCGACTGGTGTTG-3'), probe-3 (5'-CCATGAGATTCAACAG-3'), probe-4 (5'-CCTCCCCAGGACCCTCCCAA-3') and probe-5 (5'-CTGTGGGAGAACATAGGGTGAGA-3'). The probes were 5'-end labelled using T4 polynucleotide kinase (TaKaRa Bio) with [γ-^{32}P] ATP (6000Ci/mmol) at 37°C for 4 h.

Cloning of cleavage products

rDICER-processed RNAs (1 pmol) were separated on 7 M urea-denaturing 15% polyacrylamide gels, then the gel was stained by SYBR Gold (Invitrogen). The band around 23 nt was excised from the gel and purified as described above. The purified RNA was cloned by the Small RNA cloning kit (TaKaRa Bio) and sequenced by capillary sequencing.

5'-end labelling of the transcript

For the 5'-end labelling, RNA (45 pmol) was dephosphorylated with CIP at 37°C for 60 min. The reaction was inactivated by phenol-chloroform extraction and precipitated by sodium acetate-ethanol at -20°C. The pellet was resuspended in an appropriate volume of water. The dephosphorylated transcript was 5' end-labelled using T4 polynucleotide kinase (TaKaRa Bio) with [γ-^{32}P] ATP (3000Ci/mmol) at 37°C for 4 h. The 5'-end labeled transcript was PAGE-purified as described above and the RNA pellet was resuspended in water at a final concentration of approximately 0.5 pmol/μl. One microliter of this was used for the processing reaction by rDICER. These processed samples were run on 7.5 M urea-denaturing 20% polyacrylamide gels in 1x TBE buffer with RNA molecular marker or the products of alkaline hydrolysis of the same RNA molecule. The alkaline hydrolysis ladder was generated by incubating the labelled RNA in alkaline hydrolysis buffer (Ambion) at 100°C for 10 min. The signals were detected by autoradiography and quantified using ImageJ software (National Institutes of Health; http://rsb.info.nih.gov/ij/). The signal intensities were calculated as the mean of pixel value of selected area.

Additional material

Additional file 1: Supplementary information.

Acknowledgements

We thank Drs. Yasuhiro Tomaru, Timo Lassmann and Masanori Suzuki for their helpful discussion. We also thank Dr. Junichi Yano (Nippon Shinyaku Co. LTd., Kyoto) for the gift of materials. We acknowledge to RIKEN GeNAS for their support of our sequencing data production.
This work was supported by a Research Grant for the RIKEN Omics Science Center from the Ministry of Education, Culture, Sports, Science and Technology of Japan to YH.

Author details

[1]RIKEN Omics Science Center, 1-7-22 Suehiro-cho, Tsurumi-ku, Yokohama 230-0045, Japan. [2]Cancer Stem Cell Project, National Cancer Center Research Institute, 5-1-1 Tsukiji, Chuo-ku, Tokyo 104-0045, Japan. [3]Department of Biological Science and Technology, Tokyo University of Science, 2641 Yamazaki, Noda, Chiba 278-8510, Japan. [4]PREST, Japan Science and Technology Agency, 4-1-8 Honcho Kawaguchi, Saitama 332-0012, Japan.

Authors' contributions

YA conceived the study, designed and performed experiments and drafted the manuscript. YM and AM participated in the experimental design and performed experiments. RK and JC participated in the experimental design and purified recombinant FLAG-DICER fusion proteins. AMB, HS and KM participated in the design of the study and revised the manuscript. YH designed the research project, provided funding, supervised the study and critically reviewed the manuscript. All authors read and approved the final manuscript.

Received: 21 June 2010 Accepted: 9 February 2011
Published: 9 February 2011

References

1. Sontheimer EJ: **Assembly and function of RNA silencing complexes.** *Nat Rev Mol Cell Biol* 2005, **6(2)**:127-138.
2. Kim VN, Han J, Siomi MC: **Biogenesis of small RNAs in animals.** *Nat Rev Mol Cell Biol* 2009, **10(2)**:126-139.
3. Jinek M, Doudna JA: **A three-dimensional view of the molecular machinery of RNA interference.** *Nature* 2009, **457(7228)**:405-412.
4. Denli AM, Tops BB, Plasterk RH, Ketting RF, Hannon GJ: **Processing of primary microRNAs by the Microprocessor complex.** *Nature* 2004, **432(7014)**:231-235.
5. Gregory RI, Yan KP, Amuthan G, Chendrimada T, Doratotaj B, Cooch N, Shiekhattar R: **The Microprocessor complex mediates the genesis of microRNAs.** *Nature* 2004, **432(7014)**:235-240.
6. Han J, Lee Y, Yeom KH, Nam JW, Heo I, Rhee JK, Sohn SY, Cho Y, Zhang BT, Kim VN: **Molecular basis for the recognition of primary microRNAs by the Drosha-DGCR8 complex.** *Cell* 2006, **125(5)**:887-901.
7. Lund E, Guttinger S, Calado A, Dahlberg JE, Kutay U: **Nuclear export of microRNA precursors.** *Science* 2004, **303(5654)**:95-98.
8. Gregory RI, Chendrimada TP, Cooch N, Shiekhattar R: **Human RISC couples microRNA biogenesis and posttranscriptional gene silencing.** *Cell* 2005, **123(4)**:631-640.

9. Lee Y, Hur I, Park SY, Kim YK, Suh MR, Kim VN: **The role of PACT in the RNA silencing pathway.** *EMBO J* 2006, **25(3)**:522-532.
10. MacRae IJ, Ma E, Zhou M, Robinson CV, Doudna JA: **In vitro reconstitution of the human RISC-loading complex.** *Proc Natl Acad Sci USA* 2008, **105(2)**:512-517.
11. Tahbaz N, Kolb FA, Zhang H, Jaronczyk K, Filipowicz W, Hobman TC: **Characterization of the interactions between mammalian PAZ PIWI domain proteins and Dicer.** *EMBO Rep* 2004, **5(2)**:189-194.
12. Schwarz DS, Hutvagner G, Du T, Xu Z, Aronin N, Zamore PD: **Asymmetry in the assembly of the RNAi enzyme complex.** *Cell* 2003, **115(2)**:199-208.
13. Winter J, Jung S, Keller S, Gregory RI, Diederichs S: **Many roads to maturity: microRNA biogenesis pathways and their regulation.** *Nat Cell Biol* 2009, **11(3)**:228-234.
14. Khvorova A, Reynolds A, Jayasena SD: **Functional siRNAs and miRNAs exhibit strand bias.** *Cell* 2003, **115(2)**:209-216.
15. Yoda M, Kawamata T, Paroo Z, Ye X, Iwasaki S, Liu Q, Tomari Y: **ATP-dependent human RISC assembly pathways.** *Nat Struct Mol Biol* 2010, **17(1)**:17-23.
16. Tomari Y, Matranga C, Haley B, Martinez N, Zamore PD: **A protein sensor for siRNA asymmetry.** *Science* 2004, **306(5700)**:1377-1380.
17. Tomari Y, Du T, Zamore PD: **Sorting of Drosophila small silencing RNAs.** *Cell* 2007, **130(2)**:299-308.
18. Wang HW, Noland C, Siridechadilok B, Taylor DW, Ma E, Felderer K, Doudna JA, Nogales E: **Structural insights into RNA processing by the human RISC-loading complex.** *Nat Struct Mol Biol* 2009, **16(11)**:1148-1153.
19. Tomari Y, Zamore PD: **Perspective: machines for RNAi.** *Genes Dev* 2005, **19(5)**:517-529.
20. Hu HY, Yan Z, Xu Y, Hu H, Menzel C, Zhou YH, Chen W, Khaitovich P: **Sequence features associated with microRNA strand selection in humans and flies.** *BMC Genomics* 2009, **10**:413.
21. Burroughs AM, Ando Y, de Hoon MJ, Tomaru Y, Nishibu T, Ukekawa R, Funakoshi T, Kurokawa T, Suzuki H, Hayashizaki Y, *et al*: **A comprehensive survey of 3' animal miRNA modification events and a possible role for 3' adenylation in modulating miRNA targeting effectiveness.** *Genome Res* 2010, **20(10)**:1398-1410.
22. Tan GS, Garchow BG, Liu X, Yeung J, Morris JPt, Cuellar TL, McManus MT, Kiriakidou M: **Expanded RNA-binding activities of mammalian Argonaute 2.** *Nucleic Acids Res* 2009, **37(22)**:7533-7545.
23. Sakurai K, Amarzguioui M, Kim DH, Alluin J, Heale B, Song MS, Gatignol A, Behlke MA, Rossi JJ: **A role for human Dicer in pre-RISC loading of siRNAs.** *Nucleic Acids Res* 2010.
24. MacRae IJ, Doudna JA: **Ribonuclease revisited: structural insights into ribonuclease III family enzymes.** *Curr Opin Struct Biol* 2007, **17(1)**:138-145.
25. Zhang H, Kolb FA, Jaskiewicz L, Westhof E, Filipowicz W: **Single processing center models for human Dicer and bacterial RNase III.** *Cell* 2004, **118(1)**:57-68.
26. Macrae IJ, Zhou K, Li F, Repic A, Brooks AN, Cande WZ, Adams PD, Doudna JA: **Structural basis for double-stranded RNA processing by Dicer.** *Science* 2006, **311(5758)**:195-198.
27. MacRae IJ, Zhou K, Doudna JA: **Structural determinants of RNA recognition and cleavage by Dicer.** *Nat Struct Mol Biol* 2007, **14(10)**:934-940.
28. Zhang H, Kolb FA, Brondani V, Billy E, Filipowicz W: **Human Dicer preferentially cleaves dsRNAs at their termini without a requirement for ATP.** *EMBO J* 2002, **21(21)**:5875-5885.
29. Flores-Jasso CF, Arenas-Huertero C, Reyes JL, Contreras-Cubas C, Covarrubias A, Vaca L: **First step in pre-miRNAs processing by human Dicer.** *Acta Pharmacol Sin* 2009, **30(8)**:1177-1185.
30. Ruby JG, Jan CH, Bartel DP: **Intronic microRNA precursors that bypass Drosha processing.** *Nature* 2007, **448(7149)**:83-86.
31. Okamura K, Hagen JW, Duan H, Tyler DM, Lai EC: **The mirtron pathway generates microRNA-class regulatory RNAs in Drosophila.** *Cell* 2007, **130(1)**:89-100.
32. Berezikov E, Chung WJ, Willis J, Cuppen E, Lai EC: **Mammalian mirtron genes.** *Mol Cell* 2007, **28(2)**:328-336.
33. Babiarz JE, Ruby JG, Wang Y, Bartel DP, Blelloch R: **Mouse ES cells express endogenous shRNAs, siRNAs, and other Microprocessor-independent, Dicer-dependent small RNAs.** *Genes Dev* 2008, **22(20)**:2773-2785.
34. Glazov EA, Kongsuwan K, Assavalapsakul W, Horwood PF, Mitter N, Mahony TJ: **Repertoire of bovine miRNA and miRNA-like small regulatory RNAs expressed upon viral infection.** *PLoS One* 2009, **4(7)**:e6349.
35. Chiang HR, Schoenfeld LW, Ruby JG, Auyeung VC, Spies N, Baek D, Johnston WK, Russ C, Luo S, Babiarz JE, *et al*: **Mammalian microRNAs: experimental evaluation of novel and previously annotated genes.** *Genes Dev* 2010, **24(10)**:992-1009.
36. Starega-Roslan J, Krol J, Koscianska E, Kozlowski P, Szlachcic WJ, Sobczak K, Krzyzosiak WJ: **Structural basis of microRNA length variety.** *Nucleic Acids Res* 2011, **39(1)**:257-268.
37. Tam OH, Aravin AA, Stein P, Girard A, Murchison EP, Cheloufi S, Hodges E, Anger M, Sachidanandam R, Schultz RM, *et al*: **Pseudogene-derived small interfering RNAs regulate gene expression in mouse oocytes.** *Nature* 2008, **453(7194)**:534-538.
38. Watanabe T, Totoki Y, Toyoda A, Kaneda M, Kuramochi-Miyagawa S, Obata Y, Chiba H, Kohara Y, Kono T, Nakano T, *et al*: **Endogenous siRNAs from naturally formed dsRNAs regulate transcripts in mouse oocytes.** *Nature* 2008, **453(7194)**:539-543.
39. Maida Y, Yasukawa M, Furuuchi M, Lassmann T, Possemato R, Okamoto N, Kasim V, Hayashizaki Y, Hahn WC, Masutomi K: **An RNA-dependent RNA polymerase formed by TERT and the RMRP RNA.** *Nature* 2009, **461(7261)**:230-235.
40. Burroughs AM, Ando Y, Hoon ML, Tomaru Y, Suzuki H, Hayashizaki Y, Daub CO: **Deep-sequencing of human Argonaute-associated small RNAs provides insight into miRNA sorting and reveals Argonaute association with RNA fragments of diverse origin.** *RNA Biol* 2011.
41. Azuma-Mukai A, Oguri H, Mituyama T, Qian ZR, Asai K, Siomi H, Siomi MC: **Characterization of endogenous human Argonautes and their miRNA partners in RNA silencing.** *Proc Natl Acad Sci USA* 2008, **105(23)**:7964-7969.
42. Elbashir SM, Martinez J, Patkaniowska A, Lendeckel W, Tuschl T: **Functional anatomy of siRNAs for mediating efficient RNAi in Drosophila melanogaster embryo lysate.** *EMBO J* 2001, **20(23)**:6877-6888.
43. Okada C, Yamashita E, Lee SJ, Shibata S, Katahira J, Nakagawa A, Yoneda Y, Tsukihara T: **A high-resolution structure of the pre-microRNA nuclear export machinery.** *Science* 2009, **326(5957)**:1275-1279.
44. Sinkkonen L, Hugenschmidt T, Filipowicz W, Svoboda P: **Dicer is associated with ribosomal DNA chromatin in mammalian cells.** *PLoS One* 2010, **5(8)**: e12175.
45. Kimura R, Yoda A, Hayashizaki Y, Chiba J: **Novel ELISA using intracellularly biotinylated antigen for detection of antibody following DNA immunization.** *Jpn J Infect Dis* 2010, **63(1)**:41-48.
46. Griffiths-Jones S: **The microRNA Registry.** *Nucleic Acids Res* 2004, , **32 Database:** D109-111.
47. Griffiths-Jones S, Grocock RJ, van Dongen S, Bateman A, Enright AJ: **miRBase: microRNA sequences, targets and gene nomenclature.** *Nucleic Acids Res* 2006, , **34 Database:** D140-144.
48. Griffiths-Jones S, Saini HK, van Dongen S, Enright AJ: **miRBase: tools for microRNA genomics.** *Nucleic Acids Res* 2008, , **36 Database:** D154-158.
49. Sato K, Hamada M, Asai K, Mituyama T: **CENTROIDFOLD: a web server for RNA secondary structure prediction.** *Nucleic Acids Res* 2009, , **37 Web Server:** W277-280.

doi:10.1186/1471-2199-12-6
Cite this article as: Ando *et al.*: Two-step cleavage of hairpin RNA with 5' overhangs by human DICER. *BMC Molecular Biology* 2011 **12**:6.

Biol. Chem., Vol. 392, pp. 299–304, April 2011 • Copyright © by Walter de Gruyter • Berlin • New York. DOI 10.1515/BC.2011.035

Minireview

RNA-dependent RNA polymerases in RNA silencing

Yoshiko Maida[1] and Kenkichi Masutomi[1,2,*]

[1]Division of Cancer Stem Cell, National Cancer Center Research Institute, 5-1-1 Tsukiji, Chuo-ku, Tokyo 104-0045, Japan
[2]PREST, Japan Science and Technology Agency, 4-1-8 Honcho Kawaguchi, Saitama 332-0012, Japan

*Corresponding author
e-mail: kmasutom@ncc.go.jp

Abstract

RNA-dependent RNA polymerases (RdRPs) synthesize double-stranded RNAs that are processed into small RNAs and mediate gene silencing. Viral RdRPs and cellular RdRPs show little structural homology to each other. Cellular RdRPs play key roles in RNA silencing by producing complementary strands for target RNAs via Dicer-dependent and -independent mechanisms. Although the existence of a functional mammalian homolog of RdRP has long been predicted, traditional approaches to identify such enzymes were unsuccessful. Recently, human telomerase reverse transcriptase, a polymerase closely related to viral RdRPs, has been shown to function as an RdRP and contributes to RNA silencing *in vivo*. These findings suggest that endogenous small interfering RNAs are produced by several mechanisms in eukaryotes.

Keywords: heterochromatin; human telomerase reverse transcriptase (hTERT); RNA component of mitochondrial RNA processing endoribonuclease (RMRP); RNA silencing; small interfering RNA (siRNA).

Introduction

RNA-dependent RNA polymerases (RdRPs) catalyze the formation of complementary RNA strands from single-stranded RNAs. In the beginning of evolution, all organisms used RNA as their genomes and RdRPs probably played pivotal roles for successive rounds of life cycle. RdRPs were identified from RNA viruses in the early 1960s (Baltimore et al., 1963), whereby RNA genomes encode viral RdRPs for the replication and transcription of their genomes. The discovery of eukaryotic RdRPs further revealed important functions of RdRPs *in vivo*. The first eukaryotic RdRP activity was found in Chinese cabbage in 1971 (Astier-Manifacier and Cornuet, 1971). Subsequently, the homologs were identified in other plants (Boege and Heinz, 1980), fungi (Cogoni and Macino, 1999) and nematodes (Smardon et al., 2000). These eukaryotic RdRPs are categorized as cellular RdRPs different from viral RdRPs, and the studies have revealed that cellular RdRPs play key roles in the regulation of gene expression through the RNA silencing mechanism.

The first report describing the RNA silencing phenomenon was published in 1928, before RNAs had been described. In the paper, Wingard described tobacco plants in which only the initially infected leaves were necrotic and diseased owing to tobacco ring spot virus, whereas the upper leaves had become asymptomatic and resistant to secondary infection, suggesting the acquisition of immunity to the virus (Wingard, 1928). This phenomenon was called 'recovery', and we now know that the 'recovery' from the virus disease involves RNA silencing (Covey et al., 1997). RNA silencing has been shown to be involved in various eukaryotic processes, such as defense against viruses and transposable elements, and developmental regulations. RNA silencing is a sequence-specific gene-regulatory mechanism, in which small RNAs, derived from precursor double-stranded RNAs (dsRNAs), repress the targeted gene expression transcriptionally and/or post-transcriptionally. In the organisms that possess RdRPs, the precursor dsRNAs are endogenously produced from the template single-stranded RNAs through the RdRP activity. In this review, we summarize the structural basis of RdRPs and the functions of RdRPs in gene regulation.

Structural and biochemical features of RdRP

There are two major groups of RdRP: viral RdRPs and cellular RdRPs. Viral and cellular RdRPs share little sequence homology. The crystal structures of viral RdRPs are similar to those of retroviral reverse transcriptases, and they share a structure resembling a closed 'right hand' containing palm, thumb and finger domains (Sousa, 1996). The palm domain structure is particularly conserved and contains four sequence motifs preserved in all of these polymerases, indicating the fundamental importance of these structural elements in the enzymatic function of the polymerases (van Dijk et al., 2004). The core of the 'palm' structure consists of two α-helices and a four-stranded antiparallel β-sheet, shared among numerous nucleic acids polymerases with RNA recognition motif.

Viral RdRPs initiate minus-strand RNA synthesis by two different mechanisms: *de novo* and primer-dependent initiation (van Dijk et al., 2004). *de novo* initiation, also known as primer-independent initiation, is widely used in RNA viruses for complete replication of viral genomes. Several RNA viruses initiate RNA synthesis using either nucleotide or uridylylated protein primers. The nucleotide primers used in primer-dependent initiation can be divided into two groups. One type is the orthodox primers binding to complementary

template RNA. This type of primer includes the oligonucleotide primers and the 5′ end of capped cellular mRNA (cap-snatched) primers. Another is the 3′ terminus of the template RNA that folds back as hairpin loop (back-priming). RNA viruses can use one or more priming mechanisms for RNA synthesis (van Dijk et al., 2004).

RdRPs are present in one or more copies in a wide range of eukaryotes, from early-branching parabasalids, such as *Giardia*, to multicellular forms, including plants, fungi, yeast and nematods (Table 1). These cellular RdRPs are encoded by *RDR* genes. Phylogenetic and protein motif analyses revealed a wide distribution of *RDR* homologs in eukaryote from protists to multicellular organisms, with no detectable prokaryotic or viral homologs (Zong et al., 2009). By contrast, no *RDR* homologs have been identified in vertebrate and insect genomes, even though these organisms also have RNA-mediated silencing mechanisms. Cellular RdRPs share the catalytic double-psi β-barrel (DPBB) domain, containing a signature metal-coordinating motif, with the universally conserved β′ subunit of DNA-dependent RNA polymerase (Salgado et al., 2006). For example, the RdRP of *Neurospora crasse*, QDE-1, has two DPBB motifs on a single polypeptide chain and it forms dimer for polymerase reaction (Salgado et al., 2006). The highly conserved region in the DPBB domain of cellular RdRPs includes the DbDGD motif (b is a bulky residue), and the similar DxDGD motif is conserved in the β′ subunit of DNA-dependent RNA polymerases. The DxDGD motif has been shown to be essential for cellular RdRP activity. Although the motif is reminiscent of the metal-binding GDD motif (motif C) of the viral RdRPs, each RdRP belongs to different superfamilies of nucleic acid polymerases, suggesting early branching of these polymerases in evolution. In principle, RDR proteins could mediate both primer-dependent and primer-independent RNA silencing (Sugiyama et al., 2005; Salgado et al., 2006). The primer-independent process can be seen in various organisms in the production of endogenous secondary small interfering RNAs (siRNAs) (Aoki et al., 2007), and the RNA products synthesized in this manner possess 5′-triphosphate termini, whereas siRNAs generated through the cleavage of long dsRNAs via RNase III enzymes share 5′-monophosphate structure (Aoki et al., 2007) (Figure 1A and B).

Roles of cellular RdRPs in RNA silencing

Cellular RdRPs play important roles in both transcriptional and post-transcriptional gene silencing (Figure 1). Plants have six *RDR*s (*RDR1–RDR6*) (Wassenegger and Krczal, 2006), and each of them is involved in different gene silencing mechanisms. *RDR1* and *RDR6* are induced upon the cellular defense against exogenous invaders, such as viruses, viriods and trangenes. Antiviral immunity in plants is conceptualized into three phases: initiation, amplification and systemic spread. In initiation, DICER-LIKE (DCL) proteins cleave dsRNAs of viral replicative products into primary siRNAs. Following initiation, RDR1 and RDR6 amplify the silencing signals via catalyzing the synthesis of new viral dsRNAs, which are processed into secondary viral siRNAs by DCLs. This RDR-dependent antiviral silencing resulted in more than 20-fold amplification of viral siRNAs (Wang et al., 2010). *RDR6* is also involved in post-transcriptional gene silencing. Post-transcriptional gene silencing is occasionally observed in plants carrying multiple copies of transgene constructs. Extensive primary transcription of trans-

Table 1 RNA-dependent RNA polymerases (RdRPs) in various organisms.

Organism	RdRP	Characteristic functions and products in gene silencing
Fungus		
Schizosaccharomyces pombe	Rdp1	PTGS, TGS
Neurospora crassa	QDE-1	PTGS, qiRNA
	Two others	
Plant		
Arabidopsis thaliana	RDR1	PTGS
	RDR2	TGS, RdDM
	RDR6	PTGS, ta-siRNA
	Three others	
Nematode		
Caenorhabditis elegans	EGO-1	PTGS, TGS, 22G-RNA
	RRF-1	PTGS, 22G-RNA
	RRF-3	PTGS, 26G-RNA
	One other	
Fruit fly		
Drosophila melanogaster	D-elp1	TGS
Mammal		
Homo sapiens	hTERT	PTGS

PTGS, post-transcriptional gene silencing; TGS, transcriptional gene silencing; qiRNA, QDE-2-interacting small RNA; RdDM, RNA-directed DNA methylation; ta-siRNA, *trans*-acting siRNA.

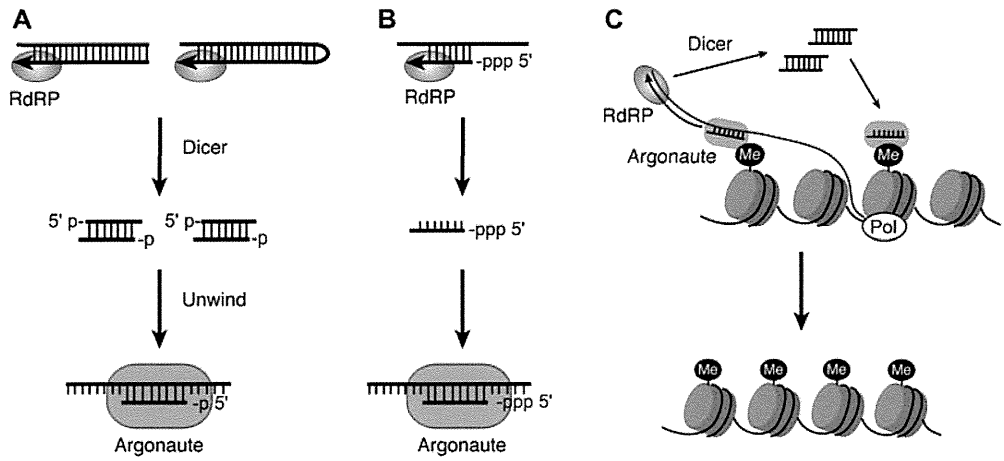

Figure 1 Common features of eukaryotic RdRP-dependent gene silencing pathways.
(A) Dicer-dependent functional small RNA synthesis. RdRPs produce long double-stranded RNAs, and the RNAs are cleaved into small double-stranded RNAs by Dicer. Argonautes load one of the strands for targeting. (B) Dicer-independent functional small RNA synthesis. RdRPs directly synthesize functional small RNAs *de novo*, independent of Dicer. (C) Heterochromatin formation. RdRPs produce antisense RNA strands for the transcripts from heterochromatic regions. Small RNAs from the regions guide histone H3K9 methylation.

genes leads to an accumulation of aberrant transgene mRNAs, which are decapped and/or unpolyadenylated (Luo and Chen, 2007). The aberrant RNAs are transcribed into dsRNA by RDR6, and subsequently processed into 21-bp siRNAs. The AGO1-bound siRNAs hybridize with complementary RNAs, both transgenes and related endogenous genes, thereby cleaving and downregulating the target RNAs. RDR6 amplifies post-transcriptional gene silencing through secondary dsRNA synthesis in a primer-dependent and primer-independent manner (Luo and Chen, 2007).

Transposable elements in eukaryotic genomes are typically silenced via the epigenetic mechanism. The plant *RDR2* genes are involved in the processes of RNA-dependent DNA methylation (RdDM) and RNAi-mediated heterochromatin formation. RdDM is triggered by the presence of nuclear dsRNAs, which are processed into 24-nt siRNAs via DCL3. The 24-nt siRNAs hybridize to the transcripts from methylated DNAs, and work as the guides for *de novo* methylation of DNA and histone H3K9 as well as RDR2-mediated secondary dsRNA production, which is required to maintain RdDM (Wassenegger and Krczal, 2006).

Plants have a unique class of endogenous siRNA named *trans*-acting siRNA (Allen et al., 2005; Cuperus et al., 2010). In *Arabidopsis*, the biogenesis of *trans*-acting siRNAs is initiated by miRNA-guided cleavage of *TAS* transcripts; *TAS1* and *TAS2* are cleaved by the AGO1-miR173 complex, *TAS3* is cleaved by the AGO7-miR390 complex, and *TAS4* is cleaved by the AGO1-miR828 complex. The resulting cleaved fragments are transformed into dsRNAs through primer-independent RNA synthesis of RDR6, and the dsRNAs are sequentially processed into phased *trans*-acting siRNA by DCL4. The miRNAs triggering biogenesis of *trans*-acting siRNAs are rather limited, and Cuperrus and co-workers recently reported that only miRNA in 22-nt length can contribute to the pathway, although most of the miRNAs in *Arabidopsis* are 21-nt (Cuperus et al., 2010).

Apart from plants with functionally different six RdRPs, non-plant eukaryotes encode fewer RdRPs and each RdRP manages more than one function of plant RdRPs. In the fission yeast *Schizosaccharomyces pombe*, a single homolog of plant RdRP (Rdp1) is associated with both RNAi and RNA-mediated heterochromatin formation (Wassenegger and Krczal, 2006). The centromeric repeats of the yeast genome form heterochromatin, whereas they are not completely silenced and transcribed by Pol II. The nascent transcripts from the centromeric region become the platforms for the RNA-induced transcriptional silencing (RITS) complex, which contains Ago1 loading the complementary siRNA. The RITS complex recruits RNA-dependent RNA polymerase complex (RDRC) containing Rdp1 to the centromere, and the RDRC promotes dsRNA synthesis from the transcripts, leading to the amplification of centromeric siRNAs. The RITS complex also recruits the Clr4-Rik1-Cul4 complex to the centromeric repeats, which mediates histone H3K9 methylation and heterochromatin formation (Sugiyama et al., 2005).

A filamentous fungus *Neurospora crassa* encodes an RdRP named QDE-1, which plays a key role in transgene-induced gene silencing (quelling) (Makeyev and Bamford, 2002). QDE-1 produces extensive RNA strands either in template-length or ~9–21-nt length (Makeyev and Bamford, 2002; Wassenegger and Krczal, 2006), which could contribute to Dicer-dependent or -independent silencing mechanisms, respectively. Recently, a new type of siRNA named QDE-2-interacting small RNA (qiRNA) was detected in *Neurospora*. The induction of qiRNA is triggered by DNA damage, and the RNA specifically corresponds to ribosomal DNA (rDNA). The production of qiRNA depends on QDE-1 and DCLs, suggesting precursor dsRNA formation through QDE-1, but RNA polymerase I, which is responsible for the transcription of rRNAs. Surprisingly, the precursor aberrant RNA of qiRNAs was transcribed from rDNA by QDE-1 itself through its DNA-dependent RNA polymerase activity,

and subsequently the dsRNAs were generated from the aberrant RNAs by the same polymerase (Lee et al., 2009).

RNAi was first described in *Caenorhabditis elegans*. The worm encodes multiple RdRP genes: i.e., *ego-1*, *rrf-1*, *rrf-3* and others. An essential feature of the RNAi pathways in *C. elegans* is the amplification of gene silencing signals via the endogenous generation of secondary siRNAs (Pak and Fire, 2007; Sijen et al., 2007). In the worm, primary siRNAs are formed from long 'trigger' dsRNAs through the processing of Dicer, and they bind to the target as guides for the recruitment of RdRPs. The RdRP on the targeted RNA synthesizes abundant complementary short RNAs *de novo* (Pak and Fire, 2007; Sijen et al., 2007), which are directory loaded onto Argonaute and function as secondary siRNAs. The protein complexes including either EGO-1 or RRF-1 generate characteristic secondary siRNAs named 22G-RNAs, which are 22-nt RNAs with a strong bias of 5′ guanosine (Claycomb et al., 2009). 22G-RNA/Argonaute complexes promote target degradation, silencing of transposable and repetitive elements, and chromosomal segregation. RRF-3 contributes to the generation of 26G-RNA (Gent et al., 2010), and it was reported that 26G-RNA/Argonaute complex worked as a guide for the following 22G-RNA synthesis (Gent et al., 2010).

Mammalian RdRP

RdRPs play an indispensable role in RNAi pathways of many model organisms; however, cellular RdRP homologs are not encoded in vertebrates, including human, and it was believed that vertebrates had evolutionally lost endogenous RNAi mechanisms that depend on the siRNA synthesis via RdRPs. Although cellular RdRP coded in the genome has not been identified, a polymerase rooted with viral RdRP remains in human. Telomerase is a ribonucleoprotein complex that elongates telomeres. The minimal essential component of this enzyme consists of the catalytic subunit named TERT (telomerase reverse transcriptase) and the template RNA called TERC (telomerase RNA component). TERT catalyzes telomere synthesis through its RNA-dependent DNA polymerase (reverse transcriptase) activity using TERC as the RNA template. Phylogenetic and structural analysis of TERT revealed that TERT shares the structure resembling 'right hand' and is closely related to RdRPs of RNA viruses as well as retroviral reverse transcriptases (Nakamura et al., 1997; Gillis et al., 2008) (Figure 2A).

We searched for RNA binding partners of TERT and identified RNA component of mitochondrial RNA processing endoribonuclease (RMRP) as the novel binding partner of hTERT (Maida et al., 2009). RMRP is a non-coding snoRNA of 267-nt in length, and it is mutated in hereditary cartilage and hair hypoplasia (Ridanpaa et al., 2001). The hTERT-RMRP complex exhibited RdRP activity, using RMRP as a template, and synthesized complementary strand of RMRP *in vitro* and *in vivo*. The result suggests that hTERT forms an RdRP with binding RNAs. The dsRNA produced by the hTERT-RMRP complex was in the shape of a long hairpin.

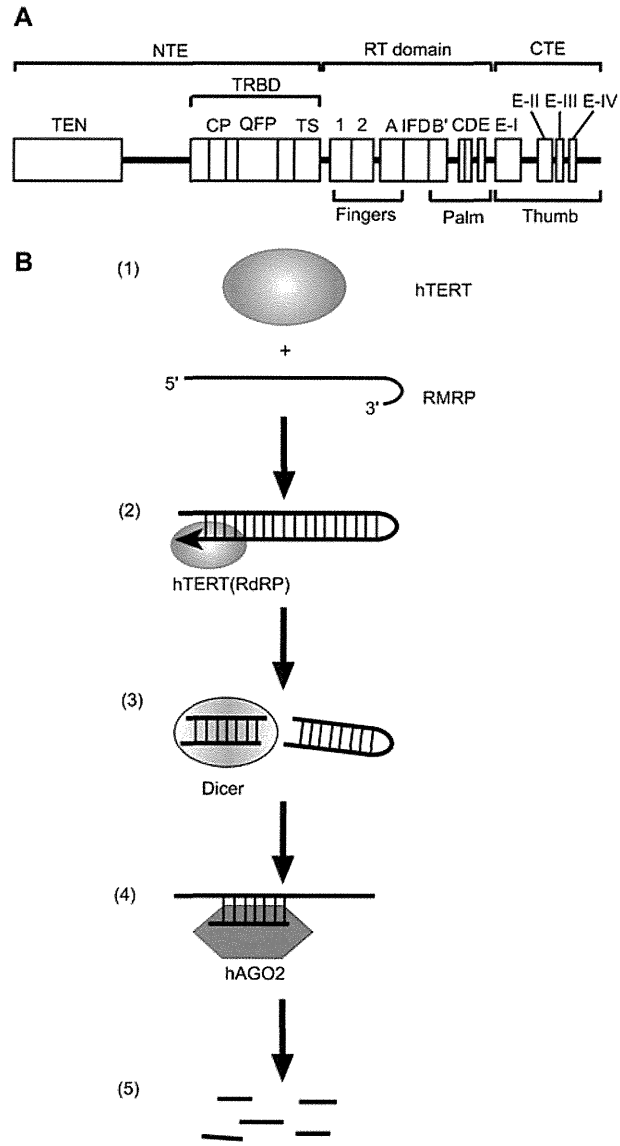

Figure 2 hTERT-mediated RNA silencing.
(A) Structure of hTERT. hTERT consists of a N-terminal extension (NTE), a catalytic reverse transcriptase (RT) domain and a C-terminal extension (CTE). NTE includes the telomerase essential N-terminal (TEN) domain and telomerase RNA-binding domain (TRBD), which contains the telomere-specific motifs CP, QFP and TS. The RT domain consists of evolutionally conserved seven motifs (1, 2, A, B′, C, D and E) and the insertion in fingers domain (IFD). CTE contains four motifs (E-I, E-II, E-III and E-IV). The fingers, palm and thumb domains are also indicated. (B) hTERT interacts with RMRP (1) and synthesizes antisense strand of RMRP via its RdRP activity through the back-priming mechanism (2). The hairpin-shaped long dsRNA is processed into small dsRNA by Dicer (3). One strand of the unwound small dsRNA is loaded onto hAGO2 (4) and targets RMRP for post-transcriptional silencing (5).

Because hTERT and RMRP did not require additional primers or ligases to generate the hairpin-shaped RNA product, hTERT started the elongation of antisense RMRP strand just after the 3′ end of sense RMRP, using back-priming. We further investigated whether the hTERT-dependent dsRNA

synthesis triggered RNA silencing in human cells *in vivo*. As seen in other model organisms, the long dsRNA with sense and antisense sequences of RMRP was processed into short dsRNA of 22-nt in length in a Dicer-dependent manner. Moreover, the one strand of the short dsRNA was loaded onto human AGO2, indicating the short dsRNA is a siRNA. The expression level of both endogenous and forcedly expressed RMRP was negatively regulated by the expression of either hTERT or Dicer, suggesting the downregulation mechanism of RMRP via post-transcriptional gene silencing (Figure 2B). These findings indicate that human retains endogenous RNAi mechanism, in which the RdRP activity of hTERT plays a key role in generating functional dsRNAs.

Recently, Kaprenov and co-workers provided additional support for the existence of a mammalian RdRP (Kapranov et al., 2010). They found a new class of gene termini-associated human RNAs, which showed extremely interesting structural characters; the RNAs were ~50-nt in length, and they had non-genetically encoded 5′ poly(U) tails as well as antisense sequences of the 3′ untranslated regions. The 5′ poly(U) tails were just followed by the antisense sequences of the very 3′ ends of known mRNAs. Based on the unique structures of the RNAs, the authors speculated the possibility of a novel RNA copying mechanism, in which RdRP produces antisense RNAs from the poly(A) tail of human mRNAs.

In addition, other proteins, such as RNA polymerase II (Lehmann et al., 2007), could also exhibit similar activities. Indeed, the RdRP in *Drosophila* was indentified from the RNA polymerase II core elongator complex subunit with no conserved amino acid domains compared with canonical cellular RdRPs (Lipardi and Paterson, 2009). The authors speculated that the human homolog of *Drosophila* RdRP, human IKAP protein, also has RdRP activity.

Conclusions and perspectives

The discovery of RNAi mechanisms has changed our understanding of the role of RNA in regulating gene expression. Many types of small non-coding RNAs, including endogenous siRNAs, contribute to the gene regulation transcriptionally and post-transcriptionally. Cellular RdRPs are indispensable to generate endogenous siRNAs in RNAi of model organisms. Although mammals have no homologs of cellular RdRPs and they have been long believed to have lost endogenous RNAi systems, our recent findings revealed that h-TERT has RdRP activity and plays a role in RNA silencing. Other groups also reported indirect evidence suggesting functional human RdRPs. These novel findings indicate that endogenous RNAi mechanisms are essential and highly preserved throughout the species, and RdRP-mediated gene regulatory mechanisms might control even more extensive events than we have imagined.

TERT and *IKAP* homologs are conserved in many eukaryotes including the model organisms with canonical cellular RdRPs. At present, it is unknown whether these novel RdRPs also function in the model organisms or not. If this is the case, the endogenous RNAi biology in these model organisms regulated by another pathway could exist. If the novel RdRPs are specific for high organisms, this could bring another simple question: why they lost canonical RdRPs? Future investigations about functional diversity of the non-canonical RdRPs in RNAi could provide us with some suggestions about this question.

RNAi has enormous potential for the treatment of many genetic and acquired diseases. Even the proteins lacking ligand-binding domains or sharing high degrees of structural homology to untargeted proteins as well as disease-causing RNAs can be targeted by the sequence-specific binding of the functional small RNAs in RNAi. Currently, several RNAi-based therapeutic approaches using exogenous siRNAs are under evaluation in clinical trials. Because hTERT is specifically and highly expressed in malignant cells, hTERT-mediated endogenous RNAi induction could become a promising novel approach in RNAi-based cancer therapeutics with reduced adverse effects in normal cells. Further functional and biochemical analysis of hTERT and other presumable human RdRPs could expand the therapeutic option for many diseases.

Acknowledgments

We thank Dr. William C. Hahn for critical reading of the manuscript and members of the Masutomi laboratory for discussions.

References

Allen, E., Xie, Z., Gustafson, A.M., and Carrington, J.C. (2005). microRNA-directed phasing during trans-acting siRNA biogenesis in plants. Cell *121*, 207–221.

Aoki, K., Moriguchi, H., Yoshioka, T., Okawa, K., and Tabara, H. (2007). *In vitro* analyses of the production and activity of secondary small interfering RNAs in *C. elegans*. EMBO J. *26*, 5007–5019.

Astier-Manifacier, S. and Cornuet, P. (1971). RNA-dependent RNA polymerase in Chinese cabbage. Biochim. Biophys. Acta *232*, 484–493.

Baltimore, D., Eggers, H.J., Franklin, R.M., and Tamm, I. (1963). Poliovirus-induced RNA polymerase and the effects of virus-specific inhibitors on its production. Proc. Natl. Acad. Sci. USA *49*, 843–849.

Boege, F. and Heinz, L.S. (1980). RNA-dependent RNA polymerase from healthy tomato leaf tissue. FEBS Lett. *121*, 91–96.

Claycomb, J.M., Batista, P.J., Pang, K.M., Gu, W., Vasale, J.J., van Wolfswinkel, J.C., Chaves, D.A., Shirayama, M., Mitani, S., Ketting, R.F., et al. (2009). The Argonaute CSR-1 and its 22G-RNA cofactors are required for holocentric chromosome segregation. Cell *139*, 123–134.

Cogoni, C. and Macino, G. (1999). Gene silencing in *Neurospora crassa* requires a protein homologous to RNA-dependent RNA polymerase. Nature *399*, 166–169.

Covey, S.N., Al-Kaff, N.S., Lángara, A., and Turner, D.S. (1997). Plants combat infection by gene silencing. Nature *385*, 781–782.

Cuperus, J.T., Carbonell, A., Fahlgren, N., Garcia-Ruiz, H., Burke, R.T., Takeda, A., Sullivan, C.M., Gilbert, S.D., Montgomery, T.A., and Carrington, J.C. (2010). Unique functionality of 22-nt

miRNAs in triggering RDR6-dependent siRNA biogenesis from target transcripts in *Arabidopsis*. Nat. Struct. Mol. Biol. *17*, 997–1003.

Gent, J.I., Lamm, A.T., Pavelec, D.M., Maniar, J.M., Parameswaran, P., Tao, L., Kennedy, S., and Fire, A.Z. (2010). Distinct phases of siRNA synthesis in an endogenous RNAi pathway in *C. elegans* soma. Mol. Cell *37*, 679–689.

Gillis, A.J., Schuller, A.P., and Skordalakes, E. (2008). Structure of the *Tribolium castaneum* telomerase catalytic subunit TERT. Nature *455*, 633–637.

Kapranov, P., Ozsolak, F., Kim, S.W., Foissac, S., Lipson, D., Hart, C., Roels, S., Borel, C., Antonarakis, S.E., Monaghan, A.P., et al. (2010). New class of gene-termini-associated human RNAs suggests a novel RNA copying mechanism. Nature *466*, 642–646.

Lee, H.C., Chang, S.S., Choudhary, S., Aalto, A.P., Maiti, M., Bamford, D.H., and Liu, Y. (2009). qiRNA is a new type of small interfering RNA induced by DNA damage. Nature *459*, 274–277.

Lehmann, E., Brueckner, F., and Cramer, P. (2007). Molecular basis of RNA-dependent RNA polymerase II activity. Nature *450*, 445–449.

Lipardi, C. and Paterson, B.M. (2009). Identification of an RNA-dependent RNA polymerase in *Drosophila* involved in RNAi and transposon suppression. Proc. Natl. Acad. Sci. USA *106*, 15645–15650.

Luo, Z. and Chen, Z. (2007). Improperly terminated, unpolyadenylated mRNA of sense transgenes is targeted by RDR6-mediated RNA silencing in *Arabidopsis*. Plant Cell *19*, 943–958.

Maida, Y., Yasukawa, M., Furuuchi, M., Lassmann, T., Possemato, R., Okamoto, N., Kasim, V., Hayashizaki, Y., Hahn, W.C., and Masutomi, K. (2009). An RNA-dependent RNA polymerase formed by TERT and the RMRP RNA. Nature *461*, 230–235.

Makeyev, E.V. and Bamford, D.H. (2002). Cellular RNA-dependent RNA polymerase involved in posttranscriptional gene silencing has two distinct activity modes. Mol. Cell *10*, 1417–1427.

Nakamura, T.M., Morin, G.B., Chapman, K.B., Weinrich, S.L., Andrews, W.H., Lingner, J., Harley, C.B., and Cech, T.R. (1997). Telomerase catalytic subunit homologs from fission yeast and human. Science *277*, 955–959.

Pak, J. and Fire, A. (2007). Distinct populations of primary and secondary effectors during RNAi in *C. elegans*. Science *315*, 241–244.

Ridanpaa, M., van Eenennaam, H., Pelin, K., Chadwick, R., Johnson, C., Yuan, B., vanVenrooij, W., Pruijn, G., Salmela, R., Rockas, S., et al. (2001). Mutations in the RNA component of RNase MRP cause a pleiotropic human disease, cartilage-hair hypoplasia. Cell *104*, 195–203.

Salgado, P.S., Koivunen, M.R., Makeyev, E.V., Bamford, D.H., Stuart, D.I., and Grimes, J.M. (2006). The structure of an RNAi polymerase links RNA silencing and transcription. PLoS Biol. *4*, e434.

Sijen, T., Steiner, F.A., Thijssen, K.L., and Plasterk, R.H. (2007). Secondary siRNAs result from unprimed RNA synthesis and form a distinct class. Science *315*, 244–247.

Smardon, A., Spoerke, J.M., Stacey, S.C., Klein, M.E., Mackin, N., and Maine, E.M. (2000). EGO-1 is related to RNA-directed RNA polymerase and functions in germ-line development and RNA interference in *C. elegans*. Curr. Biol. *10*, 169–178.

Sousa, R. (1996). Structural and mechanistic relationships between nucleic acid polymerases. Trends Biochem. Sci. *21*, 186–190.

Sugiyama, T., Cam, H., Verdel, A., Moazed, D., and Grewal, S.I. (2005). RNA-dependent RNA polymerase is an essential component of a self-enforcing loop coupling heterochromatin assembly to siRNA production. Proc. Natl. Acad. Sci. USA *102*, 152–157.

van Dijk, A.A., Makeyev, E.V., and Bamford, D.H. (2004). Initiation of viral RNA-dependent RNA polymerization. J. Gen. Virol. *85*, 1077–1093.

Wang, X.B., Wu, Q., Ito, T., Cillo, F., Li, W.X., Chen, X., Yu, J.L., and Ding, S.W. (2010). RNAi-mediated viral immunity requires amplification of virus-derived siRNAs in *Arabidopsis thaliana*. Proc. Natl. Acad. Sci. USA *107*, 484–489.

Wassenegger, M. and Krczal, G. (2006). Nomenclature and functions of RNA-directed RNA polymerases. Trends Plant Sci. *11*, 142–151.

Wingard, S.A. (1928). Hosts and symptoms of ring spot, a virus disease of plants. J. Agric. Res. *37*, 127–153.

Zong, J., Yao, X., Yin, J., Zhang, D., and Ma, H. (2009). Evolution of the RNA-dependent RNA polymerase (RdRP) genes: duplications and possible losses before and after the divergence of major eukaryotic groups. Gene *447*, 29–39.

Received September 30, 2010; accepted December 1, 2010

Maintenance of tumor initiating cells of defined genetic composition by nucleostemin

Naoko Okamoto[a,b], Mami Yasukawa[a], Christine Nguyen[c,d], Vivi Kasim[a], Yoshiko Maida[a], Richard Possemato[c], Tatsuhiro Shibata[e], Keith L. Ligon[c], Kiyoko Fukami[b], William C. Hahn[c,e,1], and Kenkichi Masutomi[a,f,1]

[a]Division of Cancer Stem Cell, National Cancer Center Research Institute, 5-1-1 Tsukiji, Chuo-ku, Tokyo 104-0045, Japan; [b]Laboratory of Genome and Biosignal, Tokyo University of Pharmacy and Life Science, 1432-1 Horinouchi, Hachioji, Tokyo 192-0392, Japan; [c]Department of Medical Oncology, Dana–Farber Cancer Institute and Department of Medicine, Brigham and Women's Hospital and Harvard Medical School, Boston, MA 02115; [d]Broad Institute, Harvard University and Massachusetts Institute of Technology, Cambridge, MA 02142; [e]Cancer Genomics Project, Center for Medical Genomics, National Cancer Center Research Institute, 5-1-1 Tsukiji, Chuo-ku, Tokyo 104-0045, Japan; and [f]Precursory Research for Embryonic Science and Technology (PREST), Japan Science and Technology Agency, 4-1-8 Honcho Kawaguchi, Saitama 332-0012, Japan

Edited by Neal F. Lue, Weill Cornell Medical College, New York, NY, and accepted by the Editorial Board June 7, 2011 (received for review October 12, 2010)

Recent work has identified a subset of cells resident in tumors that exhibit properties similar to those found in normal stem cells. Such cells are highly tumorigenic and may be involved in resistance to treatment. However, the genes that regulate the tumor initiating cell (TIC) state are unknown. Here, we show that overexpression of either of the nucleolar GTP-binding proteins nucleostemin (NS) or GNL3L drives the fraction of genetically defined tumor cells that exhibit markers and tumorigenic properties of TICs. Specifically, cells that constitutively express elevated levels of NS or GNL3L exhibit increased TWIST expression, phosphorylation of STAT3, expression of genes that induce pluripotent stem cells, and enhanced radioresistance; in addition, they form tumors even when small numbers of cells are implanted and exhibit an increased propensity to metastasize. GNL3L/NS forms a complex with the telomerase catalytic subunit [human telomerase reverse transcriptase (hTERT)] and the SWItch-Sucrose NonFermentable (SWI-SNF) complex protein brahma-related gene 1 (BRG1), and the expression of each of these components is necessary to facilitate the cancer stem cell state. Together, these observations define a complex composed of TERT, BRG1, and NS/GNL3L that maintains the function of TICs.

Both embryonic and organ-specific stem cells are characterized by the ability to self-renew and to differentiate into specialized cell types. Recent work has identified a subset of cells in tumors that exhibit properties similar to those found in normal stem cells (1–3). Such tumor initiating cells (TICs) or cancer stem cells are characterized by the capacity for unlimited self-renewal and the ability to differentiate into multiple cell types. Moreover, such cells are highly tumorigenic (4), show resistance to chemotherapy and/or radiotherapy (5–7), and may contribute to metastasis (8–11).

TICs are defined operationally. Specifically, such cells exhibit the ability to form tumors when placed in limiting numbers in animal hosts (4, 12). Although some cancer stem cells express particular cell surface receptors, the expression of such markers is not exclusive to TICs and no universal cancer stem cell markers have been identified. Indeed, recent evidence suggests that not all tumors may harbor such TICs (12, 13). Given the potential role for such cells in tumor initiation, progression, and response to treatment, defining the molecular alterations that program cancer stem cells is essential not only to identify such cells but to understand their contribution to malignant transformation.

The nucleolar GTP-binding protein nucleostemin (NS) and its closely related family member GNL3L are expressed at high levels in ES cells (14, 15), and NS has been proposed as a marker for TICs in highly aggressive brain tumors (16). NS has been reported to regulate cell proliferation through a direct interaction with p53 (14). Specifically, recent studies have shown that expression of NS and/or GNL3L delays the onset of cellular senescence by negatively regulating telomeric repeat-binding factor 1 (TRF1) stability (17) and that depletion of NS causes G1 arrest in a p53-dependent manner (18). However, other studies suggest that NS may also contribute to stem cell function independent of p53, because blastocysts derived from NS null mice failed to enter S phase even in the absence of p53 (19).

We hypothesized that NS may contribute directly to formation of cancer stem cells. Here, we show that the expression of NS/GNL3L increases the fraction of tumorigenic human cells that exhibit TIC properties.

Results

NS and GNL3L Regulate TIC Behavior. To examine whether endogenous NS was essential for the behavior of established TICs, we evaluated the consequences of suppressing *NS* in well-characterized TIC lines derived from glioblastomas (GBMs; 0308, BT145, and BT112) (20). To determine whether suppression of NS in these GBM TICs affected clonogenic neurosphere formation, a phenotype tightly correlated with tumorigenicity (21), cells were infected with either a control (short hairpin GFP) or three distinct *NS*-specific shRNAs [short hairpin NS (shNS) 1–3; Fig. 1]. We performed single-cell neurosphere formation assays and found that cells expressing the control shRNA formed neurospheres comparable to unmanipulated GBM TICs. In contrast, 0308 cells expressing *NS*-specific shRNAs displayed altered sphere-forming activity that corresponded to the degree of *NS* suppression. Specifically, cells expressing *NS*-specific shRNAs that produced the highest degree of NS suppression (shNS1 and shNS3) exhibited a significant decrease in average sphere size ($P < 0.02$; Fig. 1*A*, *Upper Left*). These cells also displayed decreased levels of neural stem cell markers CD133 and SOX2 (Fig. 1*A*, *Lower Left*). To eliminate the possibility that the observed effects were attributable to off-target effects of RNAi, we created a shRNA specific for the NS 3′UTR (shNS4) and showed that expression of this shRNA induced similar effects on the proliferation of MCF7 cells as the other *NS*-specific shRNAs and could be rescued by the expression of ectopic NS (Fig. S1 *A–C*). Moreover, suppression of NS in two other TIC lines, BT145 and BT112 (Fig. 1 *B* and *C*), also resulted in

This paper results from the Arthur M. Sackler Colloquium of the National Academy of Sciences, "Telomerase and Retrotransposons: Reverse Transcriptases That Shaped Genomes," held September 29–30, 2010, at the Arnold and Mabel Beckman Center of the National Academies of Sciences and Engineering in Irvine, CA. The complete program and audio files of most presentations are available on the NAS Web site at www.nasonline.org/telomerase_and_retrotransposons.

Author contributions: N.O., C.N., Y.M., R.P., T.S., K.F., W.C.H., and K.M. designed research; N.O., M.Y., C.N., V.K., Y.M., and R.P. performed research; N.O., M.Y., C.N., R.P., T.S., K.L.L., K.F., W.C.H., and K.M. contributed new reagents/analytic tools; N.O., M.Y., C.N., V.K., Y.M., R.P., T.S., K.L.L., K.F., W.C.H., and K.M. analyzed data; and N.O., C.N., W.C.H., and K.M. wrote the paper.

The authors declare no conflict of interest.

This article is a PNAS Direct Submission. N.F.L. is a guest editor invited by the Editorial Board.

[1]To whom correspondence may be addressed. E-mail: william_hahn@dfci.harvard.edu or kmasutom@ncc.go.jp.

This article contains supporting information online at www.pnas.org/lookup/suppl/doi:10.1073/pnas.1015171108/-/DCSupplemental.

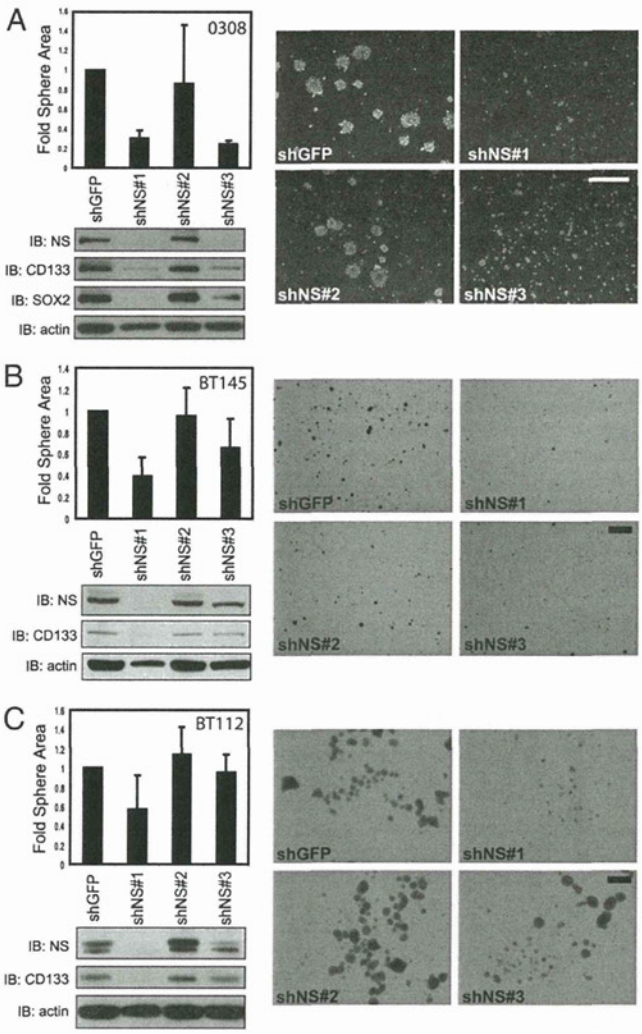

Fig. 1. NS is required for TIC function. (*A, Upper Left*) Suppression of *NS* in 0308 cells results in decreased neurosphere size. The 0308 cells expressing control or NS-specific shRNAs were grown under neurosphere promoting conditions. Triplicate images of each cell population for three independent experiments were analyzed for average neurosphere size per area (μm^2). Error bars indicate SD for three independent experiments. (*Lower Left*) Control (short hairpin GFP) and NS-specific shRNAs (shNS1–3) were introduced into 0308 cells, and endogenous NS suppression was measured by immunoblotting. IB, immunoblot; shGFP, short hairpin GFP. The expression of CD133 and SOX2 was also assessed; β-actin is shown as a loading control. (*Right*) Representative images of GBM-derived 0308 TICs containing a control or NS-specific shRNAs. (Scale bar = 250 μm.) As described in *A* performed on BT145 cells (*B*) or BT112 cells (*C*). (Scale bar = 1 mm in representative images.)

a decrease in sphere size and expression of the neural stem cell marker CD133 proportional to the degree of *NS* suppression. Together, these observations indicate that suppression of *NS* in 0308, BT145, and BT112 cells decreases the ability of these cells to form clonogenic neurospheres, and likely their tumor initiating capacity.

Although tumorigenic, human cancer cell lines derived from tumors or engineered by the expression of specific genetic elements (22) contain only a small fraction of cells that exhibit TIC behavior (4, 10, 23). To determine the effects of NS or GNL3L on the tumorigenicity of either engineered tumorigenic fibroblast [BJELR (full name: BJEHEcR-LT-Ras-ST)] and kidney epithelial (HA1ER) cells expressing the SV40 large and small T antigens, hTERT, and oncogenic H-RAS (22) or two established human cancer lines (HeLa or MCF7), we expressed NS or GNL3L at levels found in GBM-derived neurospheres and analyzed several phenotypes associated with TICs. We found that expression of either NS or GNL3L conferred the ability to form statistically larger and more numerous anchorage-independent colonies (Fig. 2 *A* and *B*) and induced enhanced tumorigenicity (Fig. 2*C*). Specifically, we observed tumor formation after the s.c. inoculation of a small number of cells overexpressing NS or GNL3L (≤500 cells), whereas cells expressing a control vector failed to form tumors. TICs have also been reported to exhibit relative resistance to ionizing radiation (5). When we irradiated BJ-hTERT, MCF7, or HeLa cells expressing a control vector, NS, or GNL3L, we found that cells expressing NS or GNL3L were more resistant to γ-irradiation (Fig. S2). These observations suggest that expression of NS or GNL3L alters the fraction of TICs present in both established and engineered cancer cell lines.

NS or GNL3L Expression Induces Markers and Pathways Associated with TICs. Several markers have been described to be expressed by TICs. When we analyzed cells overexpressing NS or GNL3L, we found increased expression of CD44 and CD133, markers associated with TICs (4, 24) (Fig. 3 *A–C*). Indeed, we found that the expression of NS or GNL3L in HeLa cells and BJ-hTERT cells induced a two- to fourfold increase in the percentage of cells expressing high levels of CD44 compared with cells expressing a control vector when we assessed either total CD44 levels (Fig. 3*A*) or CD44 expression in individual cells (Fig. 3 *B* and *C*). In addition, we confirmed that NS and GNL3L are

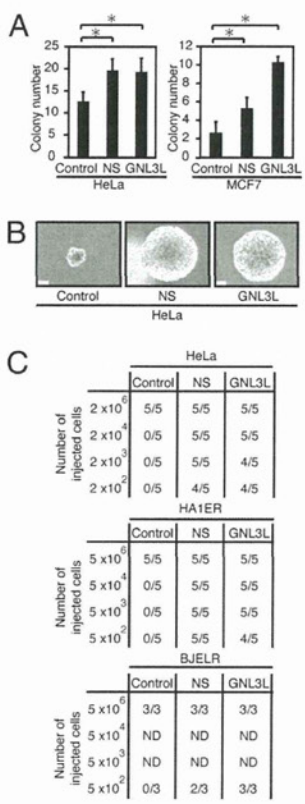

Fig. 2. Expression of NS or GNL3L induces TICs. (*A*) Anchorage-independent growth. For each cell line, 100 cells were plated and colony numbers were counted after 1 mo. The mean ± SD for three independent experiments is shown. *$P < 0.05$. (*B*) Representative micrographs demonstrate colony sizes (magnification: 100×) of HeLa cells expressing NS, GNL3L, or a control vector (control). (Scale bar = 100 μm.) (*C*) For tumorigenicity assays, the indicated numbers of cells were injected s.c. into immunodeficient mice and are reported as the number of tumors formed/number of injection sites.

significantly overexpressed in the subpopulation of several cancer cell lines previously shown (4, 23, 25) to be enriched in cells that express gene signatures related to TICs (CD44 high fraction of HeLa and CD44 high/CD24 low fraction of MDA-MB-157, MDA-MB-231, and MDA-MB-436 cells; Fig. S3 *A* and *B*).

Cell surface markers are useful tools to identify cells that exhibit cancer stem cell activity but may not unequivocally mark this cell population. We also investigated whether NS expression alters pathways implicated in the maintenance of cancer stem cells. Specifically, we determined whether expression of NS or GNL3L affected WNT/β-catenin signaling and found that expression of NS or GNL3L correlated with increased nuclear localization of the active nonphosphorylated β-catenin (Fig. 3 *D* and *E*) and induced statistically significant increased β-catenin activity as measured by reporter assay (26, 27) (Fig. 3*F*). Expression of NS or GNL3L also induced higher steady-state levels of *c-MYC*, a direct β-catenin target gene (Fig. 3*G*). The introduction of *OCT3/4*, *SOX2*, *c-MYC*, and *KLF4* into normal human and murine cells suffices to reprogram such cells into ES cells (28, 29). When we analyzed the expression of these genes in cells expressing either a control vector, NS, or GNL3L, we found that NS or GNL3L up-regulated *c-MYC*, *OCT3/4*, and *KLF4* (Fig. 3*G* and Fig. S4). These observations confirmed that the expression of NS or GNL3L induces the expression of genes associated with ES cells and cancer stem cells.

NS or GNL3L Expression Activates the Epithelial Mesenchymal Transition and Induces Metastasis. In addition to WNT/β-catenin signaling, several other pathways have been implicated in the maintenance of the cancer stem cell state. Specifically, recent evidence indicates that increased STAT3 signaling regulates the expression of the master regulator TWIST to induce epithelial mesenchymal transition (EMT) and metastasis (30). In consonance with these observations, we found that BJ-hTERT, MCF7, and HeLa cells expressing NS or GNL3L exhibited increased expression of the tyrosine phosphorylated form of STAT3 (Tyr^{705}; Fig. 4*A*) and higher levels of TWIST, SNAIL, and vimentin (Fig. 4*B*). TGF-β signaling has been implicated in the regulation of both CD44 expression and TWIST (10). To investigate whether TGF-β signaling was required for EMT in cells expressing NS or GNL3L, we treated HeLa cells expressing NS with two different TGF-β inhibitors (LY364947 and SD-208) and found that the expression of CD44 was decreased in HeLa cells expressing NS in a dose-dependent manner (Fig. 4*E*). These observations suggest that the expression of NS or GNL3L induces an EMT.

In addition, we found that tumorigenic cells expressing either NS or GNL3L exhibited increased capacity for metastasis as measured by the number of foci formed in the lungs of mice after tail vein injection of control, NS-expressing, or GNL3L-expressing cells (Fig. 4 *C* and *D*). Although this observed increase in the number of lung metastases in cells expressing NS may be attributable, in part, to the increased tumorigenicity of these cells, these observations show that NS-expressing cells exhibit several phenotypes associated with TICs (10, 11).

NS/GNL3L, BRG1, and TERT Form a Complex Necessary for TIC Function. Because TERT has been implicated in the maintenance of stem cells by both telomere-dependent (31) and telomere-independent mechanisms (32–35) and had previously been reported to interact with GNL3L (36), we determined whether the interaction of NS/GNL3L with hTERT was involved in the induction of TICs. Specifically, we isolated hTERT immune complexes and found that endogenous NS interacts with endogenous hTERT in both HeLa and 293T cells (Fig. 5*A*). To characterize the interaction of hTERT with NS or GNL3L, we used a series of TERT truncation mutants and found that the amino-terminal end of hTERT (1–531) was necessary for hTERT to interact with both NS and GNL3L (Fig. S5*A*). We also found that the conserved consensus motifs G5 and G4 present in both NS and GNL3L (37–40) were required for the interaction with hTERT (Figs. S5 *B* and *C*, and S6). These observations identify

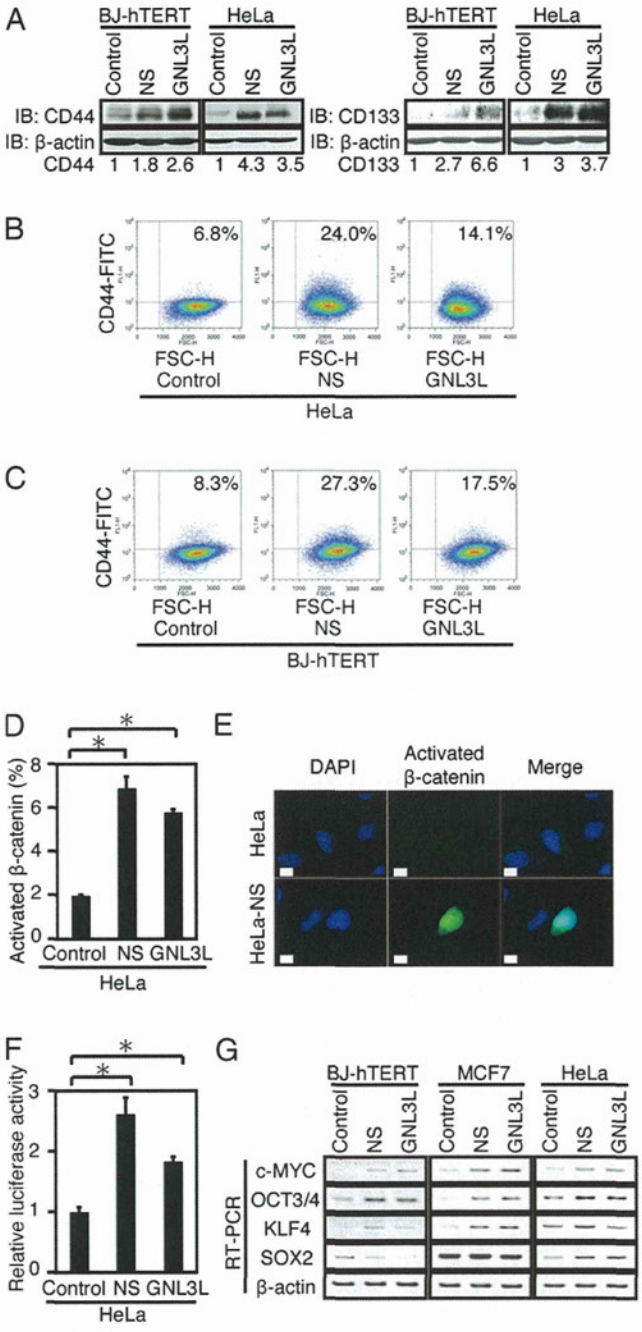

Fig. 3. Effects of NS or GNL3L on cancer stem cell markers. Effects of overexpressing NS or GNL3L on CD44 protein expression as assessed by immunoblotting (*A*) or flow cytometry (*B* and *C*). Cells were stained with FITC-conjugated anti-CD44 (Leu-44) antibody. IB, immunoblot. (*B*) Fractions of HeLa cells expressing high levels of CD44 were 6.8% (control vector), 24.0% (NS), and 14.1% (GNL3L). (*C*) Fractions of BJ-hTERT cells expressing high levels of CD44 were 8.3% (control vector), 27.3% (NS), and 17.5% (GNL3L). (*D*) Percentage of cells that harbor nuclear activated β-catenin in cells expressing a control vector, NS, or GNL3L is shown. $*P < 0.05$. (*E*) Effects of overexpressing NS or GNL3L on β-catenin function. Representative immunofluorescence images are shown. HeLa cells (*Upper*) and HeLa cells expressing NS (*Lower*) were stained with an antibody that recognizes unphosphorylated (active) β-catenin and visualized with Alexa Fluor 488 (Invitrogen)-conjugated anti-mouse IgG (green, magnification: 600×); DAPI (blue) indicates DNA. (Scale bar = 10 μm.) (*F*) TOPFLASH-Luc luciferase reporter activity. A renilla luciferase expression plasmid, pRL-SV40, was used as an internal control for transfection efficiency. $*P < 0.05$. (*G*) Effects of overexpressing NS or GNL3L on the expression of *c-MYC*, *OCT3/4*, *KLF4*, and *SOX2*.

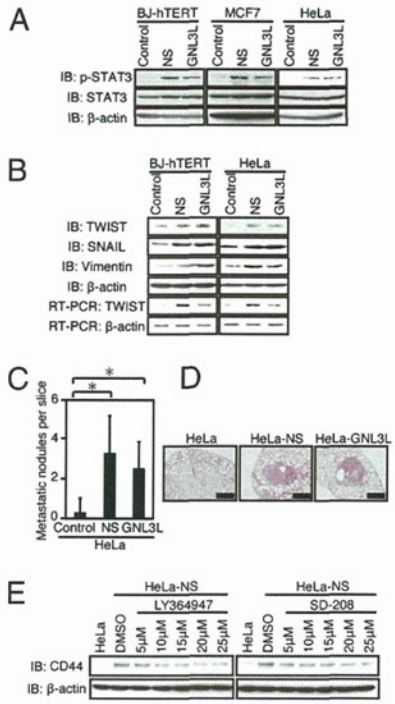

Fig. 4. Effects of NS and GNL3L on EMT and metastasis. (*A*) Effects of overexpression of NS or GNL3L on STAT3 and phospho-STAT3 (Tyr-705). IB, immunoblot. (*B*) Effects of overexpression of NS or GNL3L on TWIST, SNAIL, and vimentin expression. (*C* and *D*) Effects of overexpressing NS or GNL3L on metastasis. (*C*) Bar graph shows the number of metastatic foci found after tail vein injection. The mean ± SD for three independent experiments is shown. $*P < 0.05$. (*D*) Representative H&E images are shown (magnification: 100×). (Scale bar = 50 μm.) (*E*) Effects of TGF-β inhibitors on CD44 expression induced by NS/GNL3L. The indicated cells were treated with LY364947 or SD-208 for 24 h, followed by immunoblotting.

a specific conserved region in NS and GNL3L responsible for the interaction with hTERT.

As recently described (35), we confirmed that hTERT binds both overexpressed and endogenous BRG1 (Fig. 5 *B* and *C*). To determine whether hTERT, BRG1, and NS/GNL3L are found in the same complex, we performed two types of sequential immunoprecipitation experiments. First, we isolated FLAG–NS or FLAG–GNL3L immune complexes and confirmed that hTERT-HA was present. We then eluted these complexes with the M2 (FLAG) peptide, isolated hTERT immune complexes, and confirmed that endogenous BRG1 was present in these complexes (Fig. 5 *D* and *E*). Second, we isolated hTERT immune complexes and confirmed that BRG1 was present. We then eluted these complexes with the M2 (FLAG) peptide, isolated BRG1 immune complexes, and confirmed that endogenous NS was present (Fig. 5 *F* and *G*). These observations suggest that hTERT, BRG1, and NS or GNL3L are present in the same complex.

To determine whether the interaction of hTERT with NS/GNL3L required the telomere elongation activities of TERT, we suppressed the expression of the telomerase RNA subunit *hTERC* and found that hTERT continued to associate with NS, indicating that this interaction occurs independent of telomerase activity (Fig. S7A). Moreover, overexpression or suppression of NS or GNL3L did not affect telomerase activity or telomere length as assessed by telomere repeat amplification protocol assays or telomere restriction fragment Southern blotting (Fig. S7 *B–D*). Together, these observations suggest that complexes containing hTERT, BRG1, and NS or GNL3L do not contribute directly to telomere maintenance but, instead, drive TIC formation by regulating the activity of BRG1.

To confirm that the complex composed of hTERT, BRG1, and NS/GNL3L was involved in regulating TIC phenotypes, we assessed whether each of these components was necessary for NS-induced increase in CD44 levels. When we suppressed *hTERT* expression using *hTERT*-specific siRNAs, we failed to observe an increase in CD44 expression after expressing NS or GNL3L (Fig. 6*A*). Moreover, *BRG1* suppression reversed the increase in CD44 expression induced by NS or GNL3L expression (Fig. 6*B*). In contrast, when we suppressed *hTERC* expression using *hTERC*-specific shRNAs, we found that the expression of *hTERC* was not required for the increase in CD44 expression induced by NS or GNL3L overexpression (Fig. S7*E*). Furthermore, when we suppressed *hTERT* or *BRG1* expression, we failed to observe an increase in TWIST expression after expressing NS or GNL3L (Fig. 6 *C* and *D*). Suppression of *hTERT* or *BRG1* in cells expressing NS or GNL3L, which are markedly enriched in TICs, ablated the ability of HeLa cells expressing NS or GNL3L to form tumors (Fig. 6 *E* and *F*). Together, these observations

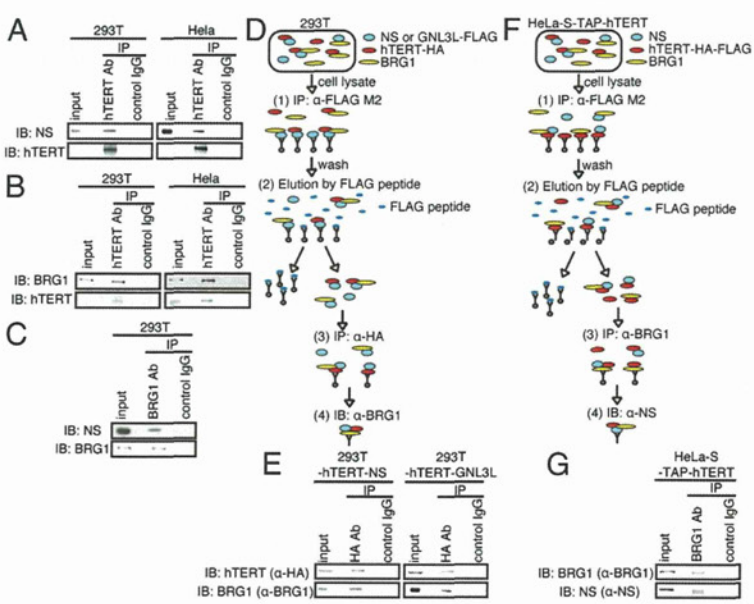

Fig. 5. NS forms a complex with hTERT and BRG1. (*A*) hTERT interacts with endogenous NS. hTERT complexes from 293T or HeLa cells were purified with an anti-hTERT antibody (Rockland), and associated proteins were subjected to SDS/PAGE and immunoblotting with an anti-NS antibody. IB, immunoblot. (*B*) hTERT interacts with endogenous BRG1. hTERT immune complexes from 293T or HeLa cells were subjected to SDS/PAGE, followed by immunoblotting with an anti-BRG1 antibody. (*C*) BRG1 interacts with endogenous NS. BRG1 complexes from 293T cells were purified by immunoprecipitation with an anti-BRG1 antibody and subjected to SDS/PAGE, followed by immunoblotting with an anti-NS antibody. Schema (*D*) and results (*E*) of the sequential immunoprecipitation using cells expressing FLAG-tagged NS or GNL3L and hTERT-HA. NS or GNL3L immune complexes were isolated and then eluted with the FLAG M2 peptide. hTERT immune complexes were then purified, and endogenous BRG1 was detected by immunoblotting. Schema (*F*) and results (*G*) of the sequential immunoprecipitation using cells stably expressing TAP-hTERT. hTERT immune complexes were isolated and eluted with the FLAG M2 peptide. Endogenous BRG1 immune complexes were isolated, and endogenous NS was analyzed by immunoblotting.

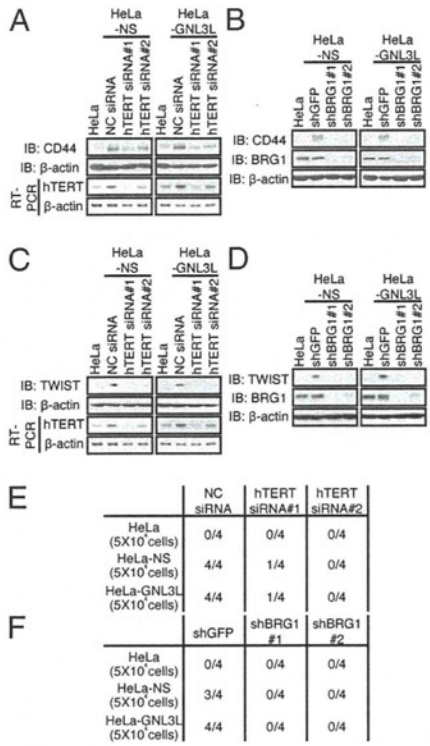

E

	NC siRNA	hTERT siRNA#1	hTERT siRNA#2
HeLa ($5X10^5$ cells)	0/4	0/4	0/4
HeLa-NS ($5X10^5$ cells)	4/4	1/4	0/4
HeLa-GNL3L ($5X10^5$ cells)	4/4	1/4	0/4

F

	shGFP	shBRG1 #1	shBRG1 #2
HeLa ($5X10^5$ cells)	0/4	0/4	0/4
HeLa-NS ($5X10^5$ cells)	3/4	0/4	0/4
HeLa-GNL3L ($5X10^5$ cells)	4/4	0/4	0/4

Fig. 6. Complex of hTERT, BRG1, and NS/GNL3L is necessary for NS-induced TIC formation. (*A*) hTERT is required for NS/GNL3L-induced increase in CD44 expression. HeLa-NS cells or HeLa-GNL3L cells expressing either a control siRNA or two independent *hTERT*-specific siRNAs were immunoblotted for CD44. IB, immunoblot. (*B*) BRG1 is required for NS/GNL3L-induced increase in CD44 expression. CD44 expression was assessed by immunoblotting in HeLa-NS cells or HeLa-GNL3L cells stably expressing either a control vector or two independent *BRG1*-specific shRNAs. (*C*) hTERT is required for NS/GNL3L-induced increase in TWIST expression. HeLa-NS cells or HeLa-GNL3L cells expressing either a control siRNA or two independent *hTERT*-specific siRNAs were immunoblotted for TWIST. (*D*) BRG1 is required for NS/GNL3L-induced increase in TWIST expression. TWIST expression was assessed by immunoblotting in HeLa-NS cells or HeLa-GNL3L cells stably expressing either a control vector or two independent *BRG1*-specific shRNAs. (*E*) hTERT is required for tumor formation by HeLa cells. The number of tumors formed/number of injection sites in HeLa-NS cells or HeLa-GNL3L cells expressing either a control siRNA or two independent *hTERT*-specific siRNAs is shown. For *E* and *F*, 5×10^4 cells were injected per mouse. NC, negative control. (*F*) BRG1 is required for tumor formation by HeLa cells expressing NS or GNL3L. HeLa-NS cells or HeLa-GNL3L cells expressing either a control vector or two independent *BRG1*-specific shRNAs are shown.

indicate that the expression of hTERT, NS/GNL3L, and BRG1 is each required to induce a TIC phenotype.

Discussion

Here, we show that expression of NS or GNL3L in genetically engineered human cancer cells confers a TIC phenotype. Tumorigenic human cells of defined genetic constitution expressing NS or GNL3L exhibited the full range of phenotypes associated with cancer stem cells, including the expression of cell surface markers such as CD44 and CD133, genes that induce induced pluripotant stem (iPS) cells, the ability to form tumors when implanted at limiting numbers, activation of an EMT program, and increased metastatic potential. Because genetically engineered human cancer cells (BJELR and HA1ER) and even established human cancer lines (HeLa and MCF7) have both TIC and non-TIC populations (Fig. S3), expressing NS or GNL3L enhances the TIC fraction.

NS was initially found to be expressed at high levels in highly proliferative multipotential cells (14, 19) as well as a subset of aggressive brain tumors (16). We found that NS and GNL3L contribute directly to the maintenance of the TIC phenotype. Prior work demonstrated that NS physically interacts with p53 and that this interaction regulates cell proliferation (14). However, it is clear that NS also contributes to stem cell function independent of p53 (19). Although we have confirmed that depletion of NS is associated with cell cycle arrest accompanied by p53 upregulation (18), the tumorigenic cells in which we expressed NS or GNL3L lack p53 function, suggesting that NS contributes to the generation of TIC independent of its regulation of p53.

TERT was recently shown to interact with GNL3L in a manner that regulated telomere length (36). We have confirmed that GNL3L and NS interact with TERT through a highly conserved region present in both of these nucleolar GTP binding proteins. However, in this setting, we failed to find evidence that the interaction of NS or GNL3L affected telomere length or telomerase activity. Instead, we found that NS or GNL3L forms a ternary complex with TERT and BRG1 in a manner that does not depend on *hTERC*. However, it remains possible that TERT–GNL3L complexes regulate telomere dynamics in other cells or conditions. These observations suggest that the NS/GNL3L–TERT–BRG1 complex operates in a telomere-independent manner to drive transcriptional programs essential to the maintenance of the TIC state. Thus, in addition to facilitating immortalization, hTERT may contribute to tumorigenicity through the NS/GNL3L–TERT–BRG1 complex by influencing the balance of cancer cells that exhibit TIC phenotypes.

Recent work indicates that TERT regulates stem cell homeostasis independent of its function at telomeres (32) and that TERT, together with BRG1, modulates stem cell homeostasis by modulating the WNT/β-catenin signaling pathway (35). We confirmed that the NS/GNL3L–TERT–BRG1 complex is essential for the maintenance of TICs. Further work will be necessary to determine whether this complex regulates normal stem cells by a similar mechanism.

In prior work, we identified a limited number of introduced genes that sufficed to convert normal human cells into tumorigenic cells (22). We and others have subsequently found specific combinations of genes mutating in spontaneously arising cancers that permitted the creation of tumorigenic human cells of a defined genetic composition (41–43). These experimental models have proven useful to decipher the cooperation between mutated genes and the discovery of new cancer genes (44, 45). However, like most established cancer cell lines, such cells formed tumors only after the implantation of a large number of cells, suggesting that additional perturbations were necessary to drive the formation of TICs. The observation that expression of NS or GNL3L in this setting leads to cells that exhibit all the phenotypes associated with cancer stem cells establishes an experimental model to define the pathways required to program the cancer stem cell state. Moreover, because the acquisition of stem cell characteristics correlates with treatment resistance and metastatic disease, these experimental models may provide the means to identify new targets to inhibit these phenotypes associated with lethal disease.

Materials and Methods

Cell Culture and Stable Expression of FLAG-NS/GNL3L and hTERT. The human cell lines 293T, MCF7, HeLa-S, HA1ER (22), and HeLa were maintained in DMEM supplemented with 10% (vol/vol) heat-inactivated FBS. BJ fibroblasts and BJELR cells were cultured as described (22). Amphotropic retroviruses were created as described (22) using the expression vector pWZL-neo, pBABE-Hygro, pWZL-neo-FLAG-NS, pWZL-neo-FLAG-GNL3L, or pBABE-Hygro-hTERT. After infection, cells were selected with neomycin (G418; 2 mg/mL) for 7 d or with hygromycin (50 mg/mL) for 3 d.

Stable Expression of shRNA. The pLKO.1-puro vector was used to express shRNAs targeting *NS*, *GNL3L*, *hTERC*, *BRG1*, and *GFP*. These vectors were used to make amphotropic lentiviruses, and polyclonal cell populations were purified by selection with puromycin (2 mg/mL).

Immunoblotting and Immunoprecipitation. Cells were lysed using a Nonidet P-40/SDS–based lysis buffer. Details concerning the conditions and antibodies used are found in *SI Materials and Methods*.

Anchorage-Independent Growth and Tumorigenicity Assays. Growth in soft agar was performed as described (22) and scored at 4 wk. For tumor experiments, cells were mixed with BD Matrigel Matrix (BD Bioscience) at 4 °C and injected s.c. in BALB/c-nu/nu mice.

Neurosphere Formation Assay. GBM-derived 0308 tumor stem cells were a gift from H. Fine (US National Institutes of Health, Bethesda, MD) and were cultured in neurobasal media (NBE; Invitrogen), 0.5× each N2 and B27 supplements (Invitrogen), and 50 ng/mL each human recombinant basic FGF and EGF (R&D Systems). BT145 and BT112 cells were cultured in NeuroCult NS-A Basal Medium (StemCell Technologies) supplemented with NeuroCult NS-A Proliferation Supplement (StemCell Technologies) and 20 ng/mL human recombinant bFGF and EGF. For shRNA experiments, cells were infected with viral supernatant diluted 1:5, spun at 930 × *g* for 30 min, and incubated at 37 °C for 1.5 h before changing to fresh media. Cells were selected with 0.4 mg/mL puromycin 24 h after infection. At 72 h after infection, the cells were trypsinized and plated to assay for neurosphere formation; after 72 h, imaging with a light microscope was performed and cell lysates were made for immunoblot analysis. To determine average sphere size, images were analyzed using ImageJ software (National Institutes of Health).

Metastasis Assay. A total of 5×10^6 cells were injected into the tail vein of BALB/c-nu/nu mice. After 4 wk, lungs were dissected to evaluate tissue morphology and to detect metastases.

ACKNOWLEDGMENTS. We thank A. Miyajima, S. Saito, S. Inanobe, S. Takahashi, T. Ochiya, and R. Takahashi for their technical assistance. We thank H. Fine for the gift of 308 cells. This work was supported, in part, by Grant-in-Aid for Young Scientists (A) 21689012 (to K.M.) from the Japanese Ministry of Education, Culture, Sports, Science, and Technology; by Third-Term Comprehensive Control Research for Cancer (K.M.) from the Japanese Ministry of Health, Labor, and Welfare; by the NOVARTIS Foundation (Japan) for the Promotion of Science (K.M.); by the Funding Program for Next Generation World-Leading Researchers (K.M.); and by Grant R01 AG23145 from the US National Institutes of Health (to W.C.H.). N.O. was supported by a Research Fellow of the Japan Society for the Promotion of Science.

1. Reya T, Morrison SJ, Clarke MF, Weissman IL (2001) Stem cells, cancer, and cancer stem cells. *Nature* 414:105–111.
2. Dalerba P, Cho RW, Clarke MF (2007) Cancer stem cells: Models and concepts. *Annu Rev Med* 58:267–284.
3. Dick JE (2009) Looking ahead in cancer stem cell research. *Nat Biotechnol* 27:44–46.
4. Al-Hajj M, Wicha MS, Benito-Hernandez A, Morrison SJ, Clarke MF (2003) Prospective identification of tumorigenic breast cancer cells. *Proc Natl Acad Sci USA* 100: 3983–3988.
5. Bao S, et al. (2006) Glioma stem cells promote radioresistance by preferential activation of the DNA damage response. *Nature* 444:756–760.
6. Rich JN, Bao S (2007) Chemotherapy and cancer stem cells. *Cell Stem Cell* 1:353–355.
7. Todaro M, et al. (2007) Colon cancer stem cells dictate tumor growth and resist cell death by production of interleukin-4. *Cell Stem Cell* 1:389–402.
8. Dalerba P, Clarke MF (2007) Cancer stem cells and tumor metastasis: First steps into uncharted territory. *Cell Stem Cell* 1:241–242.
9. Hermann PC, et al. (2007) Distinct populations of cancer stem cells determine tumor growth and metastatic activity in human pancreatic cancer. *Cell Stem Cell* 1:313–323.
10. Mani SA, et al. (2008) The epithelial-mesenchymal transition generates cells with properties of stem cells. *Cell* 133:704–715.
11. Nagahama Y, et al. (2010) PSF1, a DNA replication factor expressed widely in stem and progenitor cells, drives tumorigenic and metastatic properties. *Cancer Res* 70: 1215–1224.
12. Quintana E, et al. (2008) Efficient tumour formation by single human melanoma cells. *Nature* 456:593–598.
13. Shackleton M, Quintana E, Fearon ER, Morrison SJ (2009) Heterogeneity in cancer: Cancer stem cells versus clonal evolution. *Cell* 138:822–829.
14. Tsai RY, McKay RD (2002) A nucleolar mechanism controlling cell proliferation in stem cells and cancer cells. *Genes Dev* 16:2991–3003.
15. Baddoo M, et al. (2003) Characterization of mesenchymal stem cells isolated from murine bone marrow by negative selection. *J Cell Biochem* 89:1235–1249.
16. Tamase A, et al. (2009) Identification of tumor-initiating cells in a highly aggressive brain tumor using promoter activity of nucleostemin. *Proc Natl Acad Sci USA* 106: 17163–17168.
17. Zhu Q, Yasumoto H, Tsai RY (2006) Nucleostemin delays cellular senescence and negatively regulates TRF1 protein stability. *Mol Cell Biol* 26:9279–9290.
18. Ma H, Pederson T (2007) Depletion of the nucleolar protein nucleostemin causes G1 cell cycle arrest via the p53 pathway. *Mol Biol Cell* 18:2630–2635.
19. Beekman C, et al. (2006) Evolutionarily conserved role of nucleostemin: Controlling proliferation of stem/progenitor cells during early vertebrate development. *Mol Cell Biol* 26:9291–9301.
20. Lee J, et al. (2006) Tumor stem cells derived from glioblastomas cultured in bFGF and EGF more closely mirror the phenotype and genotype of primary tumors than do serum-cultured cell lines. *Cancer Cell* 9:391–403.
21. Vescovi AL, Galli R, Reynolds BA (2006) Brain tumour stem cells. *Nat Rev Cancer* 6: 425–436.
22. Hahn WC, et al. (1999) Creation of human tumour cells with defined genetic elements. *Nature* 400:464–468.
23. Shipitsin M, et al. (2007) Molecular definition of breast tumor heterogeneity. *Cancer Cell* 11:259–273.
24. Singh SK, et al. (2003) Identification of a cancer stem cell in human brain tumors. *Cancer Res* 63:5821–5828.
25. Ben-Porath I, et al. (2008) An embryonic stem cell-like gene expression signature in poorly differentiated aggressive human tumors. *Nat Genet* 40:499–507.
26. Miller JR, Hocking AM, Brown JD, Moon RT (1999) Mechanism and function of signal transduction by the Wnt/beta-catenin and Wnt/Ca2+ pathways. *Oncogene* 18:7860–7872.
27. Firestein R, et al. (2008) CDK8 is a colorectal cancer oncogene that regulates beta-catenin activity. *Nature* 455:547–551.
28. Takahashi K, Yamanaka S (2006) Induction of pluripotent stem cells from mouse embryonic and adult fibroblast cultures by defined factors. *Cell* 126:663–676.
29. Takahashi K, et al. (2007) Induction of pluripotent stem cells from adult human fibroblasts by defined factors. *Cell* 131:861–872.
30. Cheng GZ, et al. (2008) Twist is transcriptionally induced by activation of STAT3 and mediates STAT3 oncogenic function. *J Biol Chem* 283:14665–14673.
31. Flores I, Cayuela ML, Blasco MA (2005) Effects of telomerase and telomere length on epidermal stem cell behavior. *Science* 309:1253–1256.
32. Sarin KY, et al. (2005) Conditional telomerase induction causes proliferation of hair follicle stem cells. *Nature* 436:1048–1052.
33. Choi J, et al. (2008) TERT promotes epithelial proliferation through transcriptional control of a Myc- and Wnt-related developmental program. *PLoS Genet* 4:e10.
34. Imamura S, et al. (2008) A non-canonical function of zebrafish telomerase reverse transcriptase is required for developmental hematopoiesis. *PLoS ONE* 3:e3364.
35. Park JI, et al. (2009) Telomerase modulates Wnt signalling by association with target gene chromatin. *Nature* 460:66–72.
36. Fu D, Collins K (2007) Purification of human telomerase complexes identifies factors involved in telomerase biogenesis and telomere length regulation. *Mol Cell* 28: 773–785.
37. Daigle DM, et al. (2002) YjeQ, an essential, conserved, uncharacterized protein from Escherichia coli, is an unusual GTPase with circularly permuted G-motifs and marked burst kinetics. *Biochemistry* 41:11109–11117.
38. Leipe DD, Wolf YI, Koonin EV, Aravind L (2002) Classification and evolution of P-loop GTPases and related ATPases. *J Mol Biol* 317:41–72.
39. Meng L, Yasumoto H, Tsai RY (2006) Multiple controls regulate nucleostemin partitioning between nucleolus and nucleoplasm. *J Cell Sci* 119:5124–5136.
40. Yasumoto H, Meng L, Lin T, Zhu Q, Tsai RY (2007) GNL3L inhibits activity of estrogen-related receptor gamma by competing for coactivator binding. *J Cell Sci* 120: 2532–2543.
41. Zhao JJ, et al. (2003) Human mammary epithelial cell transformation through the activation of phosphatidylinositol 3-kinase. *Cancer Cell* 3:483–495.
42. Boehm JS, Hession MT, Bulmer SE, Hahn WC (2005) Transformation of human and murine fibroblasts without viral oncoproteins. *Mol Cell Biol* 25:6464–6474.
43. Zhao JJ, et al. (2005) The oncogenic properties of mutant p110alpha and p110beta phosphatidylinositol 3-kinases in human mammary epithelial cells. *Proc Natl Acad Sci USA* 102:18443–18448.
44. Kolfschoten IG, et al. (2005) A genetic screen identifies PITX1 as a suppressor of RAS activity and tumorigenicity. *Cell* 121:849–858.
45. Boehm JS, et al. (2007) Integrative genomic approaches identify IKBKE as a breast cancer oncogene. *Cell* 129:1065–1079.

Supporting Information

Okamoto et al. 10.1073/pnas.1015171108

SI Materials and Methods

Telomeric Repeat Amplification Protocol Assay. The telomeric repeat amplification protocol was used to detect telomere-specific reverse transcriptase activity (Millipore).

Telomere Restriction Fragment Southern Blotting. Telomere length was measured by hybridizing a ^{32}P-labeled telomeric $(CCCTAA)_3$ probe to HinfI- and RsaI-digested genomic DNA (1).

RT-PCR and Quantitative RT-PCR. Total cellular RNA was isolated using TRIzol (Invitrogen) and subjected to RT-PCR. The primers used are shown in Table S1.

The RT reaction was performed for 60 min at 42 °C, and PCR was immediately performed (94 °C for 30 s, 60 °C for 30 s, and 72 °C for 30 s). Cycle numbers for PCR are indicated in the table.

Quantitative RT-PCR was performed with a LightCycler 480 II (Roche) using LightCycler 480 SYBR Green I Master (Roche) according to the manufacturer's protocols. The primers used are shown in Table S2.

Sequences for shRNAs. The sequences used for the indicated shRNAs are shown in Table S3, where the capitalized letters represent the targeting sequences.

Transfection of siRNA. A total of 1.5 × 105 cells were plated in 24-well plates. After incubation for 24 h, cells were transfected with Lipofectamine 2000 (Invitrogen). The sequences used for the indicated siRNAs were as follows: 5′-GUGUCUGUGCCC GGGAGAATT and 5′-UUCUCCCGGGCACAGACACTT for hTERT siRNA1 and 5′-GCAUUGGAAUCAGACAGCATT and 5′-UGCUGUCUGAUUCCAAUGCTT for hTERT siRNA2. The negative control siRNA (MISSION siRNA Universal Negative Control; Sigma–Aldrich) was also used.

Immunoblotting. Cells were lysed in radioimmunoprecipitation assay (RIPA) buffer containing 1.25 % Nonidet P-40, 1.25 % (wt/vol) sodium dodecyl sulfate (SDS), 2 mM EDTA, 50 mM Tris-HCl (pH7.4), and 150 mM NaCl. After sonication, lysates were cleared of insoluble material by centrifugation at 21,000 × *g* at 4 °C for 15 min. Proteins (100 μg) were subjected to SDS/PAGE in 8% (wt/vol) polyacrylamide gels and immunoblotting. The following antibodies were used: anti-FLAG M2 Affinity Gel (Sigma–Aldrich), anti-HA11 (Covance), anti-CD133 (ab19898; Abcam), anti–β-actin AC-15 (Sigma–Aldrich), anti-human CD44H (R&D Systems), anti-GNL3 A300-600A (Bethyl Laboratories), anti-GNL3 A300-599A (Bethyl Laboratories), anti-BRG1 (gift from Ohta, Japanese National Cancer Center, Tokyo, Japan), anti-SOX2 BL6578 (Bethyl Laboratories), anti-V5 (Nacalai Tesque), anti-human TWIST (Bio Matrix Research, Inc.), antivimentin (Dako-Cytomation), anti-SNAIL ChIP Grade (Abcam), antitelomerase catalytic subunit (hTERT; Rockland), anti-Stat3 (C-20; Santa Cruz), and anti–phospho-Stat3 (Tyr705; Cell Signaling).

Immunoprecipitation. Cells were lysed in lysis buffer A (LBA) containing 0.5 % Nonidet P-40, 20 mM Trid-HCl (pH 7.4), and 150 mM NaCl. After sonication, lysates were cleared of insoluble material by centrifugation at 21,000 × *g* at 4 °C for 15 min. Twenty microliters of a prewashed 1:1 slurry of anti-FLAG M2 Affinity Gel was incubated with whole-cell lysates for 4 h or overnight at 4 °C. The anti-FLAG M2 Affinity Gel complexes were washed three times with LBA and eluted in 2× SDS loading buffer containing 20% β-mercaptoethanol, 20% (vol/vol) glycerol, 4% (wt/vol) SDS and 100 mM Tris-HCl (pH 7.4), followed by SDS/PAGE and immunoblotting. To confirm the interaction of endogenous proteins, lysates were precleared with 25 μL of TrueBlot Anti-Rabbit IgG Beads (eBioscience) for 1 h at 4 °C. After centrifugation, an anti–affinity-purified antitelomerase catalytic subunit (hTERT), anti-GST (GST; Sigma–Aldrich), or anti-BRG1 (Abcam) was incubated with precleared cell lysates for 5.5 h at 4 °C. Thirty microliters of TrueBlot Anti-Rabbit IgG Beads was then added and incubated overnight. The TrueBlot Anti-Rabbit IgG Beads complexes were washed three times with LBA and eluted in 2× SDS loading buffer, followed by SDS/PAGE and immunoblotting.

Sequential Immunoprecipitation. After sonication, lysates were cleared and 20 μL of a prewashed 1:1 slurry of anti-FLAG M2 Affinity Gel was incubated with whole-cell lysates overnight at 4 °C. The anti-FLAG M2 Affinity Gel complexes were washed three times with LBA and eluted by FLAG peptide solution (final concentration of 100 μg/mL) twice. The anti-HA antibody (F7; Santa Cruz) or anti-BRG1 antibody and Protein A Sepharose beads were incubated with eluted cell lysates overnight. The Protein A Sepharose beads complexes were washed three times with LBA and eluted in 2× SDS loading buffer, followed by SDS/PAGE and immunoblotting.

Immunofluorescence Staining. A total of 2.5×10^2 cells were seeded on a poly-L-lysine–coated glass slide. After 24 h, the cells were washed with PBS twice and permeabilized and then fixed in 3.7% (vol/vol) formaldehyde plus 2% (wt/vol) sucrose and 0.1% Triton X-100 in PBS buffer for 5 min. The cells were then washed three times with PBS and incubated with the blocking solution (1% BSA in PBS). The cells were then incubated with the anti–β-catenin (BD Transduction Laboratories) for 1 h, washed three times with PBS for 2 min, and incubated with Alexa Fluor 488 (Invitrogen) for 1 h. The slides were washed extensively with PBS and mounted with Vectashield mounting medium for immunofluorescence with DAPI (Vector Laboratories, Inc.). All matched samples were photographed (control and test) using an immunofluorescence microscope (IX81, OLYMPUS) and identical exposure times.

Reporter Assay. A total of 3×10^4 cells were plated in 24-well plates. After incubation for 24 h, cells were transfected with a pTOPFLASH-Luc reporter construct. A renilla luciferase expression plasmid, pRL-SV40, was cotransfected at a concentration of 10 ng per well as an internal control for transfection efficiency. After 48 h, cells were lysed with passive lysis buffer and assayed for luciferase activity using a Dual-Luciferase Reporter Assay System (Promega).

Flow Cytometry and Cell Sorting. Cells were incubated in PBS containing 2% (vol/vol) FBS with FITC-conjugated anti-CD44 (Leu-44) antibody (BD Bioscience), allophycocyanin (APC)-conjugated anti-human CD133 antibody (eBioscience), APC- conjugated anti-CD44 antibody (BD Bioscience), or phycoerythrin-conjugated anti-CD24 antibody (BD Bioscience). Isotype-matched murine Igs served as controls. For flow cytometry, samples were analyzed using a JSAN (Bay Bioscience). For cell sorting by flow cytometry, samples were analyzed and sorted on a BD FACSVantage SE (BD Bioscience), JSAN, or BD FACSAriaII (BD Bioscience).

Clonogenic Assay. Two hundred cells were seeded into six-well plates in triplicate and exposed to radiation after 24–48 h. Cells were allowed to proliferate for 10–12 d, trypsinized, and replated into plates to elim-